APPENDIX B. RADIONUCLIDE RELEASES, DISPERSION AND DEPOSITION

I. INTRODUCTION

B1. This appendix sets out the Committee's evaluation of information on the releases of radionuclides from the accident at the Fukushima Daiichi Nuclear Power Station (FDNPS) to the atmosphere and to the ocean and their subsequent dispersion in the environment (see chapter I of the main text of the scientific annex for the timescale of the evaluation).

B2. An overview of estimates of the radionuclide releases to the atmosphere and to the ocean, both of the total amounts and the rates of release over time, is provided in section II. The meteorological conditions that prevailed during the period when the releases to the atmosphere were greatest (11-31 March) are described in section III; the influence of these conditions on how and where the released material was dispersed in, and deposited from, the atmosphere onto the Japanese land mass and the ocean surface is illustrated. Based on these meteorological conditions and the time-dependent releases to the atmosphere, estimates have been made—using atmospheric transport, dispersion and deposition models (ATDM)—of the spatial and temporal distribution of radioactive material in the environment (that is, concentrations of radionuclides in air and deposited on the ground as a function of

time). This was done to estimate levels of radioactive material in the environment at places and times for which measurements did not exist; these measured and estimated levels underpinned the assessment of doses to the public described in appendix C. The dispersion of radioactive material released to the ocean (directly or indirectly) is described in section IV.

II. RADIONUCLIDE RELEASES

A. Releases to atmosphere

B3. The accident at FDNPS resulted in the release of large amounts of radioactive material into the environment. A large number of fission and activation products were released from the molten fuel in the reactors, generally as aerosols or in a gaseous form. Those that contributed most to the radiation exposure of members of the public and workers were isotopes of iodine, caesium, tellurium and the noble gases. The accident was classified by the Japanese Nuclear and Industrial Safety Agency (NISA) at the highest level (level 7) on the International Nuclear Event Scale (INES). The main sequence of events in each reactor that resulted in the release of radioactive material is summarized below.

1. Accident sequence

B4. The earthquake that occurred off the eastern coast of Japan at 14:46 Japan Standard Time[30] (JST) on 11 March 2011 resulted in reactors in Units 1–3 of FDNPS shutting down automatically. The three other reactors (Units 4–6) had already been shut down for routine outages and Unit 4 had been completely de-fuelled. The earthquake damaged the power transmission grids from the Shin–Fukushima electrical substation and FDNPS lost all connection with its off-site electricity supply. In addition, the tsunami inundated the FDNPS site less than one hour later and flooded a number of emergency safety systems, in particular the on-site power distribution system and the DC power supply system. Units 1, 2 and 4 lost all of their power supplies. Unit 3 initially lost its AC power followed by loss of DC power during the night of 12–13 March. The tsunami also washed away vehicles, heavy equipment and oil tanks, ruined buildings, equipment and facilities, and devastated the site more generally. This exceptional situation resulted in the melting of the reactor cores of Units 1, 2 and 3 and the substantial release of radioactive material into the atmosphere and the ocean.

B5. The main events that influenced the release of radioactive material from Units 1–3 of FDNPS (as set out in the July 2012 final report of the Investigation Committee on the Accident at the Fukushima Nuclear Power Stations of Tokyo Electric Power Company [I9], and supplemented by the 2012 report Fukushima Nuclear Accident Independent Investigation Commission of the National Diet of Japan [N2]) are summarized in table B1.

[30] In this appendix, unless specifically stated otherwise, all dates and times are given in Japan Standard Time (JST).

Table B1. Summary of the main events that influenced the release of radioactive material from Units 1–3 of FDNPS [I9, N2]

All times are JST

Date (2011)	*Unit 1*	*Unit 2*	*Unit 3*
11 March	**14:46 EARTHQUAKE**		
	Automatic shutdown (Scram[31]) Loss of external AC electricity Automatic activation of emergency diesel generators		
	14:52 Start of core cooling by isolation condenser (IC)	14:50 Start of core cooling by Reactor Core Isolation Cooling (RCIC) system	15:05 Start of core cooling by Reactor Core Isolation Cooling (RCIC) system
	15:35 MAJOR TSUNAMI		
	15:37 Loss of all electricity		15:37 Loss of AC power
	IC stopped operating following loss of all power ~20:00 Possible start of damage to core and reactor pressure vessel ~21:50 Radiation in reactor building reached levels for building to be declared off-limits ~22:00 Core likely to have been damaged to considerable degree	RCIC continued to operate for about 70 hours, but its operation could not be controlled because of lack of DC power	16:03 RCIC manually restarted; RCIC continued to operate for about 21 hours; DC power enabled measuring instruments to function correctly
12 March	02:45 Strong likelihood of reactor pressure vessel failure 04:50 First indications of off-site release detected; ambient dose equivalent rate at site boundary 1 μSv/h	Between ~04:20 and ~05:00 water source for RCIC switched to suppression chamber	11:36 RCIC and water injection into reactor stopped 12:35 High pressure coolant injection (HPCI) system started automatically and restored water level
	15:36 Explosion of hydrogen accumulated in reactor building; possible release of large amounts of radioactive material into the atmosphere; dose rates at site boundary increased to around 1 mSv/h 19:04 Fire trucks started to fill reactor with seawater	15:36 Explosion in Unit 1 caused blow-out panel in reactor building to open	~19:00 HPCI operated below allowable operating range 20:36 Reactor water level measurement devices became inoperable and water injection capacity of HPCI started to become insufficient to maintain water level

[31] A scram is a safety feature that triggers immediate shutting down of a nuclear reactor, usually by rapid insertion of control rods, either automatically or manually by the reactor operator. Also known as a "reactor trip".

Date (2011)	*Unit 1*	*Unit 2*	*Unit 3*
13 March			02:42 HPCI manually stopped, because of concern about possible damage, before confirming availability of alternative diesel-driven fire-pump system; unsuccessful attempt to restart HPCI ~02:45 Unsuccessful attempt to reduce pressure in reactor pressure vessel through safety relief valve ~06:30 to ~09:10 Likely damage to reactor pressure vessel and degradation of its containment function ~08:45 Start of venting of primary containment vessel 09:25 Start of injection of fresh water 12:20 Water tank emptied; reactor water level dropped again 13:12 Seawater injection started, but occasionally interrupted, and flow rate never sufficient to fully re-cover core
14 March		04:30 Started monitoring pressure of suppression chamber 09:00 Water injection functionality of RCIC started to degrade 12:30 RCIC failure and cessation of water injection into reactor ~13:45 to ~18:10 Possible damage to primary containment vessel ~16:34 Start of depressurization of reactor pressure vessel through safety relief valve by 18:22 Indications that core may have been completely uncovered 19:57 Seawater injection started but disrupted several times ~21:18 Failure of reactor pressure vessel containment function	11:01 Hydrogen explosion occurred in reactor building with possible release of large amounts of radioactive material 16:30 Seawater injection restarted, but sometimes interrupted
15 March		From ~07:38 Release of large amounts of radioactive materials; peak dose rate at ~09:00 about 12,000 µSv/h at site boundary 19:54 More seawater successfully injected into reactor; continued in following days with varying degrees of success as reactor pressure varied	~06:00 to ~06:12 Hydrogen explosion occurred at Unit 4 from backflow of gases vented from Unit 3

Date (2011)	*Unit 1*	*Unit 2*	*Unit 3*
20 March	Off-site power restored and Unit 1 progressively brought back under control	Off-site power restored and Unit 2 progressively brought back under control	
22 March			Off-site power restored and Unit 3 progressively brought back under control

Note: Concerns were frequently expressed during the accident over the adequacy of the cooling of the spent fuel in the storage pool of Unit 4, in particular whether the fuel may have become uncovered (due to possible earthquake damage), and thus overheated. Notwithstanding these concerns, there was no release of radioactive material to the atmosphere from the spent fuel pool. Furthermore, the hydrogen explosion which damaged Unit 4 on 15 March was caused by the backflow of gases from the venting of Unit 3 (see above).

2. Approaches to estimating the source term

B6. Estimates of the source term (that is the time-dependent release of radioactive material to the environment) were made for two main purposes:

(a) To indicate the amounts of radioactive material released to the environment;

(b) To be used, in combination with models (for example, for atmospheric and marine dispersion), as support for inferring the dispersion and deposition of radionuclides at locations in the environment where measurements were not available or could no longer be made.

Measured and estimated levels of radionuclides in the environment were used by the Committee to estimate exposure levels to members of the public (see appendix C).

B7. Estimates of the release of radioactive material to the atmosphere can be made using two complementary approaches: *(a)* based on analyses of how an accident progressed; and *(b)* based on measurements of radioactive material in the environment and using reverse or inverse methods to reconstruct their transport through the atmosphere back to the source of the release. Both approaches have their limitations and are associated with much uncertainty.

B8. The first approach, based on analyses of the progression of an accident, uses reactor simulation codes, such as MELCOR [G4], ASTEC [C5] and MAAP [E3]. The main inputs to these computer codes are *(a)* the events that are either known or are postulated to have occurred during the progression of the accident and *(b)* the characteristics of the reactors. The simulations are based on detailed modelling of the different parts of the reactor and its systems, and address all the physical and chemical phenomena involved in the course of a severe accident (for example, thermal-hydraulic conditions, the behaviour of the fuel as temperatures rise when cooling is reduced or lost, the release of radionuclides from the fuel into the reactor coolant as the fuel overheats, hydrogen production, the degradation of the reactor core as the fuel melts and how it interacts with the bottom of the reactor vessel, the retention of radionuclides in the containment and their release to the environment through any leakage paths, and so on). These computer codes were developed for, and are used extensively in, reactor safety assessments, in particular in relation to designing reactors to prevent and mitigate potential severe accidents. The uncertainty associated with the use of these codes for estimating the release of radionuclides following an actual accident is, however, much greater, not least because of the lack of specific information on key plant parameters as the accident progresses, the need to make major assumptions about the timing and nature of key events in the process, and the fact that the models still represent a considerable simplification of reality. The Fukushima Nuclear Accident Independent Investigation Commission of the National Diet of Japan [N2] expressed major reservations about the reliability of these methods, both now and in the future, because of the major uncertainties about what exactly occurred in the damaged reactors. The estimates so far published using these methods only considered releases during the first few days of the accident; this limited their usefulness for the Committee's purpose of estimating exposures, where account needed to be taken of all significant releases.

B9. The second approach is based on measurements of radioactive material in the environment and the use of reverse or inverse modelling:

(a) Reverse modelling evaluates the rates of release of radionuclides by comparing measurements of radioactive material or dose rates in the environment with estimates derived from simulations of dispersion of radionuclides in the atmosphere. Atmospheric transport, dispersion and deposition

models (ATDM) are used to estimate levels in the environment for unit release of a radionuclide. Each measurement location is considered independently and the estimate is compared with the measurement; the release is adjusted empirically to fit the measured levels. Comparisons can be made with a range of measurements of radionuclides in the environment, for example, time-dependent concentrations in air and deposition densities on the ground, dose rates, and dust samples. A weakness of this approach is that it does not take account of uncertainties or bias in the measurements, the dispersion model and the meteorological data.

(b) Inverse modelling involves a similar, but mathematically more sophisticated, approach in which the (matrix) equation relating the measured values (of concentration or deposition density of radionuclides, or dose rate) to the source term is solved by minimizing the function which includes all of the sources of technical error that contribute to differences between calculated values (derived generally by ATDM) and measured values. Technical errors are therefore explicitly taken into account.

B10. Estimates made using this second approach are also associated with much uncertainty; their quality is influenced by the availability and quality of measurements of radiation or radioactive material in the environment and of meteorological data of sufficient temporal and spatial resolution. The complexity of a release (for example, marked variation in its magnitude and characteristics such as its height, thermal energy, and chemical form with time) adds further to the uncertainty. In addition, where the source term had been estimated by reverse or inverse modelling, it was inextricably linked to and dependent on the measurement data, the meteorology and the ATDM used in its derivation; if different meteorology or ATDM had been used with the measurement data, then the resulting source term estimate could have been different. Strictly, therefore, source term estimates derived in this way would be best used to estimate environmental levels by employing the same meteorology and ATDM used in their derivation. If used with different meteorology and ATDM to predict concentrations of radionuclides in the environment, the fit with measurements could have been less good (at least at those measurement points used for the reverse or inverse modelling). The extent to which this matters in practice is the subject of ongoing scientific discussion.

3. Source term estimates

B11. Numerous estimates have been published of the release of radioactive material from FDNPS; these are summarized in table B2 in terms of the total release of two of the more radiologically important radionuclides, ^{131}I and ^{137}Cs. For each case, the method used and the date the estimate was made and/or the date of its publication are indicated. The earliest estimates were made in late March 2011, even while the accident was still progressing. Others followed in the subsequent months, with many being further refined over time as more information became available (relating to both the development of the accident and measurements in the environment), and as methods improved. This subject remains an active area for research and investigation and further improvements can be expected.

Table B2. Source terms estimated for the FDNPS accident

Strictly, the various estimates of "total release" are not all directly comparable[a]

Reference	*Date of publication*	*"Total" release[a] (PBq)*		*Approach used*	*Comments*
		^{131}I	^{137}Cs		
IRSN [I31]	22 March 2011	90	10	Accident progression	Based on limited information while the accident was still progressing. Estimates related to time period 12 to 22 March 2011
ZAMG [Z3]	22 March 2011	400	33	Reverse modelling	Based on limited information while the accident was still progressing. Estimates related to first 4 days of accident (12 to 15 March 2011 inclusive)
NISA [N13]	12 April 2011	130	6	Accident progression	Estimates made for purposes of INES assessment of accident severity
NISA [N14]	6 June 2011	160	15	Accident progression	Estimates related to time period 12 to 18 March 2011
Chino et al. [C6]	July 2011	150	13	Reverse modelling	Estimates for the period 12 to 31 March 2011 only. Based on limited data available at the time. Subsequently refined by Katata et al. [K1] and Terada et al. [T19]
NISA[b]	16 February 2012	150	8	Accident progression	Included releases only over a limited period
Stohl et al. [S11]	1 March 2012[c]	–	37	Inverse modelling	Based solely on CTBTO measurements in the northern hemisphere. Guided by a first estimate based on assumptions on the total release from the three reactors and from the spent fuel pool of Unit 4, analysed the accident sequence using MELCOR and on-site measurements of dose rate. Appeared to be an overestimate compared with most other estimates
Winiarek et al. [W15]	9 March 2012	190–380	12	Inverse modelling	Obtained similar results when using inverse modelling with and without a first estimate (used an IRSN-estimated source term as the first estimate). Source term estimate limited to releases that were partly or wholly dispersed over Japanese land mass
TEPCO [T13, T15]	24 May 2012	≈500	≈10	Reverse modelling	Based on dose rates measured by monitoring vehicles on site and considered most unlikely to be an underestimate. Estimates related to time period 12 to 31 March 2011
Terada et al. [T19]	19 June 2012	120	9	Reverse modelling	Further refinement of Chino et al. [C6] and Katata et al. [K1]. Releases over the ocean estimated by interpolation of those over the land
Mathieu et al. [M6]	June 2012	197	20.6	Forward and reverse modelling	Based on dose-rate measurements on- and off-site using IRSN codes. Source term estimate limited to releases that were partly or wholly dispersed over Japanese land mass
Katata et al. [K1]	July 2012	130	11	Reverse modelling	Refinement of Chino et al. [C6] using more extensive monitoring data during the early stages of the accident. The releases tabulated were the sums of the estimates made by Katata et al. for the period up to 17 March 2011 and by Chino et al. for the period after 17 March. For the period up to 17 March, Katata et al. estimated releases of ^{131}I and ^{137}Cs of 44 and 3.9 PBq, respectively
Hoshi and Hirano [H9]	17 September 2012	250–340	7.3–13	Accident progression	Estimates relate to period 11 to 17 March 2011

Reference	Date of publication	"Total" release[a] (PBq)		Approach used	Comments
		^{131}I	^{137}Cs		
Achim et al. [A2]	September 2012	400	10	Reverse modelling	Based solely on CTBTO measurements in the northern hemisphere. Release of ^{131}I in particulate form estimated to be 100 PBq. Estimate of total release was more uncertain and relied on assumptions about gas–particulate conversion of iodine
Kobayashi et al. [K18]	15 March 2013	200	13	Reverse modelling	Further refinement of Terada et al. [T19] to provide a better estimate (i.e. not interpolated) of radionuclides dispersed directly over the ocean. Coupled atmospheric and oceanic dispersion simulations with observed concentrations of ^{134}Cs in the Pacific Ocean
Saunier et al. [S3]	25 November 2013[d]	106	15.5	Inverse modelling	Used an original approach (using IRSN codes) to inverse modelling based solely on dose-rate measurements from 57 monitoring stations in Japan. Source term estimate limited to releases that were partly or wholly dispersed over Japanese land mass

[a] *The various estimates of "total release" are not all directly comparable. Many of the estimates of "total" release do not actually represent the total and, where appropriate, this is indicated in the comments column. Some estimates were for releases over prescribed time periods. Estimates based on reverse or inverse modelling used different approaches in estimating the releases that were dispersed wholly over the ocean: in some cases these releases were estimated by interpolating between estimates of releases that were obtained by simulating dispersion over the Japanese land mass (i.e. where environmental measurements were made); in others the component of the total release that was dispersed wholly or partially over the Japanese land mass was simply not included in the total; and in one case, environmental measurements made on land were supplemented with measurements made in ocean water in order to estimate the total release.*

[b] *Quoted in [T13, T15].*

[c] *Published online as a discussion paper on 20 October 2011.*

[d] *Published online as a discussion paper on 12 June 2013.*

B12. Given their inherent uncertainties and the fact that not all of the estimates were directly comparable (that is, some early estimates covered only the first days after the accident, whereas others integrated the release over a much longer period; and some represented the total release to the atmosphere, whereas others represented only that fraction that was partly or wholly dispersed over the Japanese land mass—see table B2), the various estimates of the releases of the two principal radionuclides spanned relatively small ranges. For ^{131}I the estimates ranged from about 100 to 500 PBq; for ^{137}Cs they ranged, in general, from about 6 to 20 PBq (albeit with some estimates based on more limited information ranging up to 40 PBq). For perspective, the releases of ^{131}I and ^{137}Cs following the Chernobyl accident were estimated at 1,760 and 85 PBq, respectively [U12], that is about factors of 10 and 5 times higher than the averages of the estimates given in table B2 for the FDNPS accident.

B13. Much greater variation was, however, apparent in the estimated temporal patterns of release and this is exemplified in figure B-I for three of the published estimates. While all three show peaks in the estimated release rate of ^{137}Cs corresponding to the main events occurring at the three reactors, these peaks were assessed to have occurred at different times, to have been of different durations, and to have differed in magnitude at particular times by more than a factor of ten.

Figure B-I. Three estimates of the pattern of release rates of ^{137}Cs over time [S3, S11, T19]

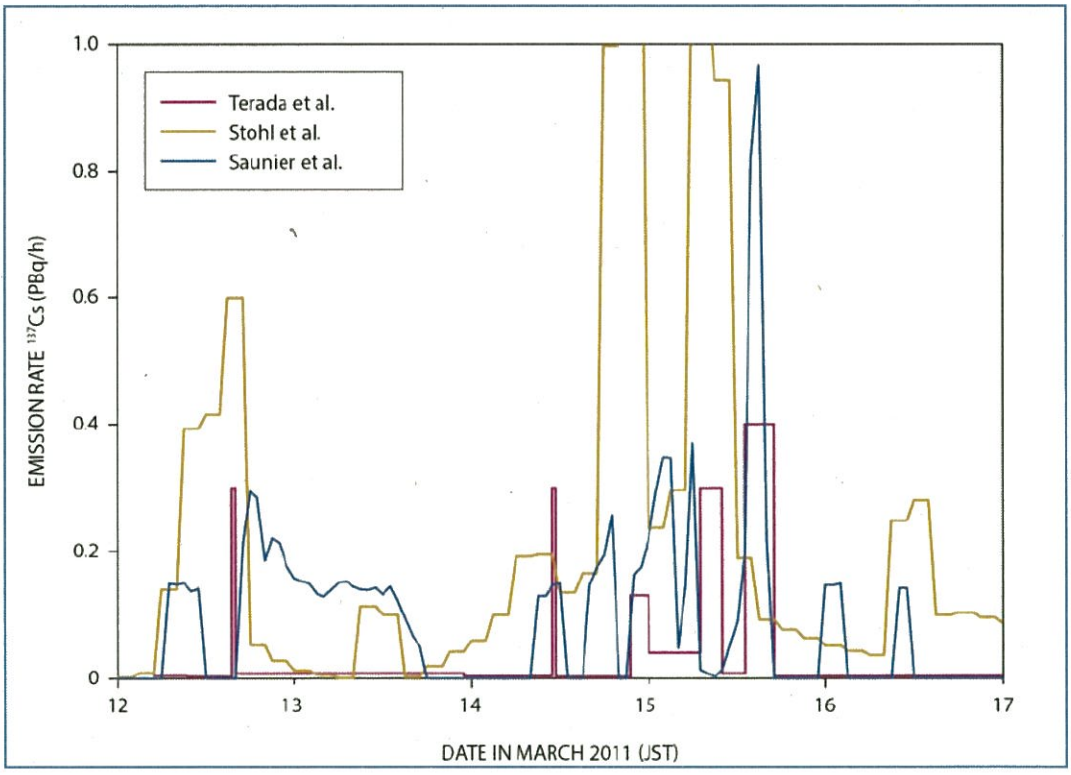

B14. The various estimates have differing strengths and weaknesses reflecting when they were made and the methods used. In general, the Committee preferred those made later because they were often refinements of earlier estimates and/or had benefited from additional information. Further, the Committee preferred estimates derived using inverse or reverse modelling, as opposed to those from analyses of accident progression for three reasons: *(a)* the former are judged to be more reliable being based on measurements of radioactive material in the environment; *(b)* the Committee acknowledged the major reservations expressed in the report by the Fukushima Nuclear Accident Independent

Investigation Commission of the National Diet of Japan [N2] on the reliability of estimates based on accident progression; and *(c)* estimates based on accident progression only covered a limited period of the release.

B15. For its purposes, the Committee had to select a source term that was best able to provide a sound basis for estimating levels of radioactive material in the environment where no measurements existed; these levels were an essential input to the subsequent estimation of doses (see chapter IV of the main annex A, and appendix C). Estimates based on reverse or inverse modelling, as opposed to simulation of accident progression, were clearly preferable in this context consequent upon them having been derived from, and optimized to fit, measurements of radioactive material in the environment. The Committee chose to use the source term estimated by Terada et al. [T19] from among those derived on the basis of reverse or inverse modelling. This was the last but one refinement in a series of estimates made by a group of Japanese scientists at JAEA [C6, K1]. It was chosen in preference to the latest refinement by Kobayashi et al. [K18] that took account of measurements of radioactive material in the Pacific Ocean in addition to those over the Japanese land mass; by contrast, Terada et al. had estimated the magnitude of releases dispersed wholly over the ocean by interpolation between releases for which measurements were available over the Japanese land mass. Adoption of the Kobayashi et al. source term by the Committee would, however, have resulted in an overestimation of the levels of radioactive material in the terrestrial environment, which would have been inconsistent with the Committee's intent of making a realistic assessment. The Committee did not consider the source term estimated by Saunier et al. [S3] because it had not yet been published at the time the choice was made; it was, however, subsequently used to test the robustness of a number of assumptions made regarding the use of the source term of Terada et al. together with ATDM simulations for estimating levels of radionuclides in the environment (see section III.E of this appendix).

B16. The releases of ^{131}I and ^{137}Cs estimated by Terada et al. lay within the ranges of published source terms in table B2, albeit at the lower ends. While they provided a sound basis for estimating the levels of radioactive material in the terrestrial environment where measurements did not exist, there were indications that they may have been underestimates of the total amounts of these radionuclides released, perhaps by a factor of up to about two because of assumptions made about the magnitude of releases dispersed wholly over the ocean (see table B2). For its purposes, the Committee had to specify a source term to provide a sound basis for estimating levels of radioactive material in the terrestrial environment where no measurements existed. With one exception (that is, for evacuees during the early stages of the accident), the levels of radionuclides in the environment estimated on the basis of the assumed source term and its subsequent dispersion in the atmosphere were not used in any absolute sense; rather, they were used in a relative sense to scale measured deposition densities of radionuclides on the ground to infer concentrations of radionuclides in the air. When used in this relative way, the scaling (and the inferred concentration in air) is relatively insensitive to plausible choices of the source term (see section E of this appendix).

B17. Terada et al. provided estimates of the releases of ^{131}I and ^{137}Cs as a function of time. These two radionuclides, together with ^{134}Cs, make by far the largest contribution to the dose received by the population. A large number of other radionuclides would also have been released in the accident and some were measured in the environment; but very few were released in sufficient amounts to contribute significantly to doses. Those that could have contributed significantly were incorporated by the Committee into the source term used, and comprised other isotopes of iodine and caesium, ^{132}Te and ^{133}Xe.

B18. The significance of very short-lived radionuclides was greatly reduced by the delay between reactor shutdown and when the first release occurred (around 14 hours). The fractional release and significance of isotopes of elements such as strontium, barium and plutonium was much lower than

those of iodine and caesium because of their much lower volatilities; this has been confirmed by measurements in the environment [N18][32].

B19. The releases of other isotopes of iodine and caesium were estimated from those of ^{131}I and ^{137}Cs by scaling with the ratio of their respective inventories in the three reactor units at shutdown and taking account of radioactive decay before the time of any release. This approach was justified because the behaviour of all isotopes of iodine (and likewise all isotopes of caesium) was the same within a given reactor and its containment system; consequently, their fractional releases (relative to their inventories at any given time) were identical. The ratios of other isotopes of iodine and caesium [N16] for each of the three units at the time of shutdown and for the three units taken as a whole are shown in table B3. The ratios differed slightly between the three units reflecting the different operating histories of the reactors; average values were assumed to apply throughout the release period when estimating the releases of these other radioisotopes. The ratio of ^{133}I to ^{131}I, corrected for radioactive decay back to the time of reactor shutdown (14:46 on 11 March 2011 JST), was derived from measurements of air samples taken between 14 and 20 March 2011 at various locations in Japan and also by the CTBTO network (figure B-II); the measured ratios are broadly in accord with the $^{133}I/^{131}I$ ratio averaged over the inventory of the three reactors. Iodine isotopes were assumed to be released in equal amounts in particulate and gaseous/elemental forms notwithstanding the wide variation over time in their relative components in measurements (contribution of particulates varying, in general, within a range of about 20% to 70%) [F7, O2]; ^{132}I produced by radioactive decay of the parent radionuclide ^{132}Te was, however, assumed to be in particulate form only (that is, the form assumed for its parent).

Table B3. Ratios of the quantities of other radionuclides to those of ^{131}I or ^{137}Cs in the three reactors at time of shutdown (14:46 on 11 March 2011 JST) [N16]

Reactor unit	*Radionuclide ratio*				
	$^{132}I/^{131}I$	$^{133}I/^{131}I$	$^{132}Te/^{137}Cs$	$^{134}Cs/^{137}Cs$	$^{136}Cs/^{137}Cs$
Unit 1	1.47	2.10	9.7	0.94	0.27
Unit 2	1.47	2.09	13.2	1.08	0.32
Unit 3	1.47	2.10	14.0	1.05	0.34
Average ratio (Units 1–3)	1.47	2.10	12.4	1.03	0.31

B20. For releases of isotopes of tellurium, however, there was no a priori reason why they should have been directly correlated with those of caesium or iodine; the chemistry, physical characteristics and behaviour in the reactors of these three elements were all different and would have influenced both the timing and magnitudes of their releases. Measured concentrations of ^{132}Te in air samples, relative to those of ^{137}Cs, are shown in figures B-III and B-IV. Figure B-III includes measurements made in Japan at different times by various research institutes; measurements from other sources were also available but showed greater variability in the ratio, raising some additional questions about their reliability. Figure B-IV contains measurements from the CTBTO network (see attachment B–1 for details); the line through the data is the ratio of the respective inventories of ^{132}Te and ^{137}Cs (corrected for radioactive decay to the time of shutdown). The measured $^{132}Te/^{137}Cs$ ratios varied considerably with time and space, typically from a value of a few to a few tens (corrected for radioactive decay to the time

[32] This situation differs markedly from that of the Chernobyl accident; less volatile elements (for example strontium and plutonium) were released, in relatively larger amounts, directly to the atmosphere as a result of the initial explosion and physical destruction of parts of the core. Such mechanisms did not occur in the accident at FDNPS, where the volatility of the elements, and the extent to which they were retained within the containment by other mechanisms (for example the suppression pool), were the principal determinants of the amounts released.

of shutdown). The data, however, were not sufficiently comprehensive or consistent to be used to estimate or model the time dependence of the release of ^{132}Te. In the absence of such data, the release of ^{132}Te relative to that of ^{137}Cs was assumed to be fixed and determined from their respective inventories in the three reactors at the time of shutdown, i.e. an average ratio of 12.4, as indicated in table B3. In broad terms this assumption was reasonable (see the comparisons between the lines and data in figures B-III and B-IV); however, this led to under- and overestimates of the release of ^{132}Te during particular release episodes, which may have had implications for the contribution of this radionuclide to estimated doses.

Figure B-II. Ratio of ^{133}I to ^{131}I in air samples taken between 14 and 20 March 2011 in Japan and by the CTBTO network (corrected for radioactive decay to time of reactor shutdown, 14:46 on 11 March 2011 JST, see attachment B–1)

The dashed line corresponds to a ratio of 2.1, the average ratio of the respective inventories of the two isotopes in the three units at shutdown [K5, O2, T7]; see attachment B–1 for CTBTO data. For Takasaki pre-detection: the data from the CTBTO station at Takasaki for the first 2 days when extraordinary preliminary signals were recorded; these data were considered to be valid for checking radionuclide ratios only

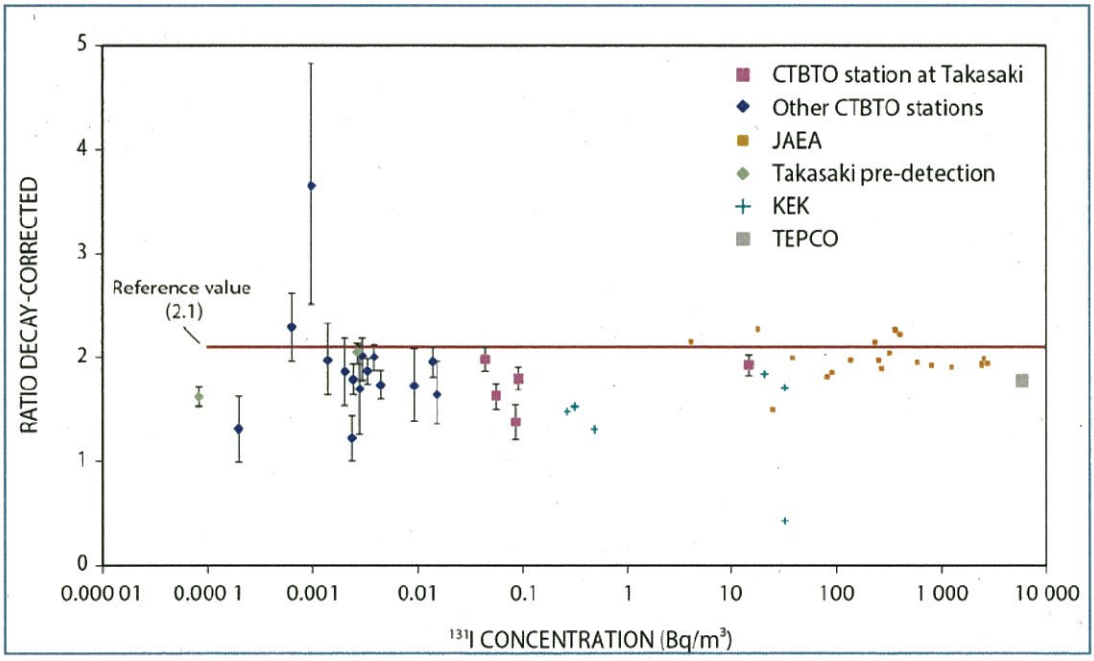

Figure B-III. Ratio of ^{132}Te to ^{137}Cs concentrations in air samples measured at various locations and times (JST) in Japan

The line represents how the ratio would vary as a function of time if the releases of ^{132}Te and ^{137}Cs had been in proportion to their respective inventories in the three units [A9, F7, J6, K5, O2]

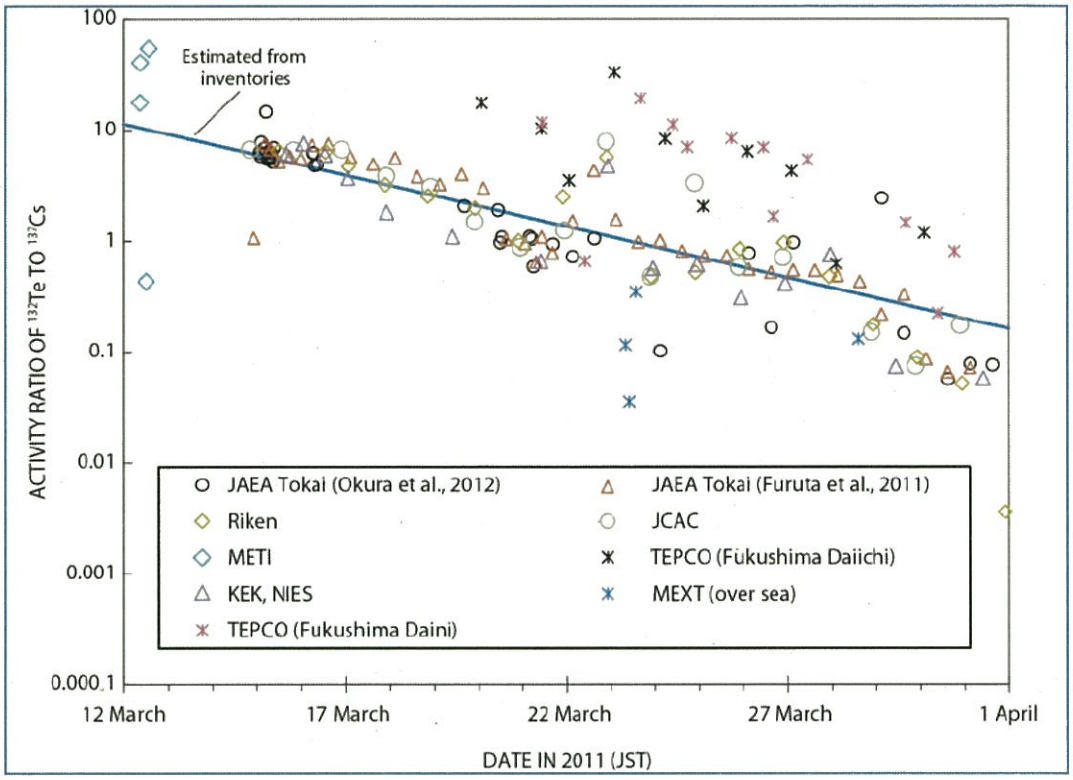

Figure B-IV. Comparison of measured concentrations of ^{132}Te and ^{137}Cs in air samples measured by the CTBTO network (corrected for radioactive decay to the time of reactor shutdown, 14:46 on 11 March 2011 JST)

See attachment B-1 for measurement data

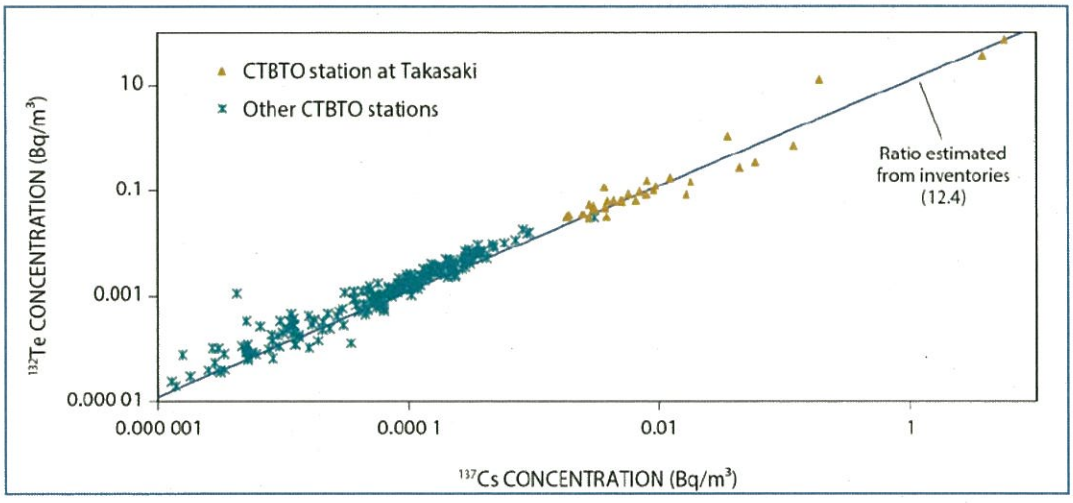

B21. For ^{133}Xe, the temporal pattern of release estimated by the updated simulation of [H10] was adopted together with the estimated inventory of this radionuclide in the three operating reactors taken from Nishihara et al. [N16]; this estimate was comparable with those of Le Petit et al. [L4] and Achim et al. [A2]. The total release of each radionuclide in the source term adopted for the purposes of this study is summarized in table B4; the time-dependent releases of the two most significant radionuclides, ^{131}I and ^{137}Cs, are shown in figures B-I and B-XVI.

B22. While most of the radioactive material was released in the period up to 17 March, releases continued for a considerable time thereafter. After the first week, the release rates gradually declined, albeit with some fluctuations over more limited periods of time (see table B5 and figure B-I). By the beginning of April, the rate of release had fallen to one thousandth or less of those during the first week; these much lower release rates persisted for many weeks afterwards, but were insignificant compared with what had gone before.

Table B4. Estimated total amounts of radiologically significant radionuclides released to atmosphere (based on [T19])

Radionuclides	*Total release to atmosphere (Bq)*	*Percentage of the inventory at reactor shutdown released (%)*
^{132}Te	2.85×10^{16}	0.33
^{131}I	1.24×10^{17}	2.1
^{132}I[a]	2.85×10^{16}	0.32
^{133}I	9.56×10^{15}	0.07
^{133}Xe	7.32×10^{18}	61
^{134}Cs	9.01×10^{15}	1.3
^{136}Cs	1.77×10^{15}	0.81
^{137}Cs	8.83×10^{15}	1.3

[a] *Direct release of ^{132}I was small compared to the ingrowth from radioactive decay of released ^{132}Te.*

Table B5. Estimated release rates to atmosphere of potentially significant radionuclides (based on [T19])

Time period in 2011 (JST)		*Duration (h)*	*Release rate (Bq/h)*							
Start	*End*		^{132}Te	^{131}I	^{132}I	^{133}I	^{133}Xe	^{134}Cs	^{136}Cs	^{137}Cs
12March 05:00	12 March 09:30	4.5	4.0×10^{13}	3.7×10^{13}	4.0×10^{13}	4.8×10^{13}	6.6×10^{15}	3.8×10^{12}	1.1×10^{12}	3.7×10^{12}
12 March 09:30	12 March 15:30	6	1.7×10^{13}	1.7×10^{13}	1.7×10^{13}	1.9×10^{13}	7.6×10^{16}	1.8×10^{12}	5.1×10^{11}	1.7×10^{12}
12 March 15:30	12 March 16:00	0.5	3.0×10^{15}	3.0×10^{15}	3.0×10^{15}	3.0×10^{15}	1.2×10^{16}	3.1×10^{14}	8.9×10^{13}	3.0×10^{14}
12 March 16:00	13 March 23:00	31	7.3×10^{13}	8.4×10^{13}	7.3×10^{13}	5.5×10^{13}	1.2×10^{17}	8.6×10^{12}	2.4×10^{12}	8.4×10^{12}
12 March 23:00	14 March 11:00	12	2.6×10^{13}	3.6×10^{13}	2.6×10^{13}	1.2×10^{13}	5.8×10^{15}	3.7×10^{12}	9.8×10^{11}	3.6×10^{12}
14 March 11:00	14 March 11:30	0.5	2.0×10^{15}	3.0×10^{15}	2.0×10^{15}	8.3×10^{14}	6.4×10^{15}	3.1×10^{14}	8.1×10^{13}	3.0×10^{14}
14 March 11:30	14 March 21:30	10	1.5×10^{13}	2.3×10^{13}	1.5×10^{13}	5.5×10^{12}	6.1×10^{15}	2.4×10^{12}	6.1×10^{11}	2.3×10^{12}
14 March 21:30	15 March 00:00	2.5	7.9×10^{14}	1.3×10^{15}	7.9×10^{14}	2.6×10^{14}	6.6×10^{15}	1.3×10^{14}	3.4×10^{13}	1.3×10^{14}
15 March 00:00	15 March 07:00	7	2.3×10^{14}	3.5×10^{14}	2.3×10^{14}	6.0×10^{13}	1.1×10^{17}	4.1×10^{13}	1.0×10^{13}	4.0×10^{13}
15 March 07:00	15 March 10:00	3	1.7×10^{15}	3.0×10^{15}	1.7×10^{15}	4.4×10^{14}	1.9×10^{17}	3.1×10^{14}	7.7×10^{13}	3.0×10^{14}
15 March 10:00	15 March 13:00	3	4.3×10^{13}	8.0×10^{13}	4.3×10^{13}	1.1×10^{13}	1.1×10^{17}	8.2×10^{12}	2.0×10^{12}	8.0×10^{12}
15 March 13:00	15 March 17:00	4	2.1×10^{15}	4.0×10^{15}	2.1×10^{15}	4.9×10^{14}	2.1×10^{17}	4.1×10^{14}	1.1×10^{14}	4.0×10^{14}
15 March 17:00	17 March 06:00	37	1.3×10^{13}	2.1×10^{14}	1.3×10^{13}	1.5×10^{13}	1.3×10^{16}	3.1×10^{12}	7.3×10^{11}	3.0×10^{12}
17 March 06:00	19 March 15:00	57	2.9×10^{13}	4.1×10^{14}	2.9×10^{13}	7.6×10^{12}		1.0×10^{13}	2.2×10^{12}	1.0×10^{13}
19 March 15:00	21 March 03:00	36	6.6×10^{13}	3.8×10^{14}	6.6×10^{13}	1.7×10^{12}		3.5×10^{13}	6.8×10^{12}	3.5×10^{13}
21 March 03:00	21 March 21:00	18	2.1×10^{13}	1.4×10^{14}	2.1×10^{13}	2.7×10^{11}		1.4×10^{13}	2.6×10^{12}	1.4×10^{13}
21 March 21:00	22 March 23:00	26	5.8×10^{12}	4.1×10^{14}	5.8×10^{12}	4.1×10^{11}		4.8×10^{12}	8.3×10^{11}	4.7×10^{12}
22 March 23:00	24 March 00:00	25	8.7×10^{12}	7.1×10^{14}	8.7×10^{12}	3.3×10^{11}		9.0×10^{12}	1.5×10^{12}	8.9×10^{12}
24 March 00:00	25 March 00:00	24	2.3×10^{12}	1.9×10^{14}	2.3×10^{12}	4.3×10^{10}		2.9×10^{12}	4.6×10^{11}	2.9×10^{12}
25 March 00:00	26 March 11:00	35	7.5×10^{11}	5.6×10^{13}	7.5×10^{11}	5.4×10^{9}		1.3×10^{12}	1.9×10^{11}	1.2×10^{12}
26 March 11:00	28 March 10:00	47	7.3×10^{10}	4.0×10^{12}	7.3×10^{10}	1.2×10^{8}		1.8×10^{11}	2.4×10^{10}	1.7×10^{11}
28 March 10:00	29 March 21:00	35	1.4×10^{12}	7.5×10^{12}	1.4×10^{12}	6.4×10^{7}		4.8×10^{12}	5.8×10^{11}	4.7×10^{12}
29 March 21:00	30 March 11:00	14	2.1×10^{12}	1.5×10^{13}	2.1×10^{12}	6.0×10^{7}		8.9×10^{12}	1.0×10^{12}	8.8×10^{12}
30 March 11:00	31 March 00:00	13	2.9×10^{13}	1.8×10^{14}	2.9×10^{13}	4.8×10^{8}		1.4×10^{14}	1.6×10^{13}	1.4×10^{14}

Time period in 2011 (JST)		Duration (h)	Release rate (Bq/h)							
Start	End		^{132}Te	^{131}I	$^{132}I^{a}$	^{133}I	^{133}Xe	^{134}Cs	^{136}Cs	^{137}Cs
31 March 00:00	31 March 22:00	22	8.0×10^{11}	2.4×10^{13}	8.0×10^{11}	3.9×10^{7}		4.6×10^{12}	5.0×10^{11}	4.5×10^{12}
31 March 22:00	2 April 09:00	35	2.2×10^{11}	1.8×10^{12}	2.2×10^{11}	1.3×10^{6}		1.7×10^{12}	1.7×10^{11}	1.6×10^{12}
2 April 09:00	4 April 09:00	48	5.5×10^{10}	1.8×10^{12}	5.5×10^{10}	3.9×10^{5}		5.9×10^{11}	5.5×10^{10}	5.8×10^{11}
4 April 09:00	7 April 17:00	80	7.8×10^{9}	7.0×10^{11}	7.8×10^{9}	2.6×10^{4}		1.4×10^{11}	1.2×10^{10}	1.4×10^{11}
7 April 17:00	13 April 23:00	150	7.2×10^{9}	7.0×10^{11}	7.2×10^{9}	1.4×10^{3}		3.5×10^{11}	2.2×10^{10}	3.5×10^{11}
13 April 23:00	1 May 00:00	409	4.5×10^{8}	7.0×10^{11}	4.5×10^{8}	6.2×10^{0}		1.7×10^{11}	6.2×10^{9}	1.8×10^{11}

[a] Direct release rate of ^{132}I is small compared to the ingrowth from radioactive decay of released ^{132}Te.

B. Releases to the ocean

B23. Radioactive material from FDNPS entered the marine environment directly and indirectly.

- Direct release into the ocean was at least known to have resulted from leakage of highly-contaminated water from a trench outside Unit 2 (discovered on 2 April 2011), and the deliberate discharge of weakly contaminated radioactive liquid waste from storage tanks; the latter were emptied to create capacity for the storage of highly contaminated water remaining in the trench (see section III below). Further releases occurred subsequently (for example in May and December 2011) but, in general, these were insignificant compared with those that occurred in the first month after the accident. In addition, groundwater, contaminated by numerous sources of radioactive material on site (e.g. leaks from storage tanks, dispersal of contaminated reactor coolant, and deposition of radionuclides released to the atmosphere), represents a continuing source of release to the ocean.

- Radioactive material entered the ocean indirectly via two routes: *(a)* most importantly, from the deposition onto the ocean surface of material released to the atmosphere and dispersed over the ocean; and *(b)* from run-off into rivers of material deposited over the land mass and transported downstream into the ocean. This latter process would continue over an extended period. Further releases could not be excluded in the future, either inadvertently (e.g. from water continuing to be released from the reactor buildings into groundwater) or as part of the waste management strategy adopted in the remediation of the FDNPS site.

B24. At the end of 2013, releases of radionuclides to the marine environment continued to be reported [N19], apparently emanating from contaminated groundwater on the FDNPS site. Several tens of per cent of the inventories of the more volatile elements (i.e. hydrogen/tritium, iodine and caesium) in the cores of the three damaged reactors had been found in stagnant water, mainly in the basement of the turbine and reactor buildings but also in surrounding areas [N15]. Less volatile elements (e.g. strontium, barium and lanthanum) had also been found but at levels that were between about a tenth to one hundredth of those for the more volatile elements in terms of their relative inventories. Monitoring results published by the Nuclear Regulation Authority [N18] indicated that these continuing release rates during 2013 were much lower than of the major releases that occurred in the immediate aftermath of the accident. Furthermore, measures were being taken to attempt to control them (e.g. the building of a containment wall between the FDNPS site and the ocean). As at the end of 2013, it was considered that the ongoing releases were unlikely to significantly affect the Committee's assessment of doses to the public. However, continued monitoring and assessment of the implications of the releases were warranted.

B25. Following the accident, numerous observations were carried out in the ocean in order to detect the presence of radionuclides released from FDNPS and have continued ever since. The operator of the station (TEPCO), the Japanese government agencies, and research laboratories from different countries (mainly Japan) collected and analysed numerous samples of water, suspended matter, sediment, and marine organisms. These measurement data are described in detail in section IV below. They were used by various authors to estimate the amounts of radionuclides released directly into the ocean. These estimates are summarized in table B6 together with estimates of the deposition on to the ocean surface from material released to atmosphere.

Table B6. Comparison of estimates of direct release to the ocean with those of deposition on the ocean surface from the atmosphere

Source of estimate (Period considered in 2011)	*Direct release to the ocean (PBq)*		*Deposition on ocean surface from the atmosphere (PBq)*	
	^{131}I	^{137}Cs	^{131}I	^{137}Cs
TEPCO [T15] (26 March–30 September)	11	3.6		
Kawamura et al. [K3] (12 March–30 April)	11[a]	4[a]	57	5
Tsumune et al. [T24] (26 March–31 May)		3.5 ± 0.7		
Bailly du Bois et al. [B2] (26 March–18 July)		27 ± 15		
Estournel et al. [E4]		0.81[b] 4.1–4.5[c] 5.5 (upper bound)		5.7–5.9 (northern Pacific Ocean)
Charette et al. [C4]		11–16		
Kobayashi et al. [K18] (12 March–1 May)	11	3.5[d]	99	7.6

[a] *21 March–30 April.* [b] *1–6 April.* [c] *12 March–30 June.* [d] *26 March–30 June.*

B26. Tsumune et al. [T24] indicated from an analysis of $^{131}I/^{137}Cs$ ratios that atmospheric inputs were responsible for concentrations in seawater measured before 26 March 2011. Atmospheric inputs would have been responsible for concentrations of ^{137}Cs ranging from 100 to 1,000 Bq/L in the vicinity of FDNPS, a few tens of becquerels per litre 10 km to the south and about 10 Bq/L at 30 km. It should be noted that this is an approximation because atmospheric deposition was not isotropic around FDNPS. The total amounts estimated by Kawamura et al. [K3] to have been deposited on the surface of the northern Pacific Ocean from the atmosphere were about 60 PBq and 5 PBq for ^{131}I and ^{137}Cs, respectively. Estournel et al. [E4] estimated that about 6 PBq of ^{137}Cs was deposited on the northern Pacific Ocean; only a small percentage (about 5%) of this amount, however, was estimated to have been deposited within a radius of 80 km of FDNPS. Kobayashi et al. [K18] estimated the deposition of ^{131}I and ^{137}Cs to be about 99 PBq and 7.6 PBq, respectively; these estimates were derived from coupling atmospheric and oceanic dispersion simulations with observed concentrations of ^{134}Cs in seawater collected from the Pacific Ocean.

B27. Several authors have used models of oceanic circulation and radionuclide dispersion in the ocean to estimate the magnitude of direct releases of radionuclides into the ocean from FDNPS. Kawamura et al. [K3] used the information published by TEPCO of the leak detected from 1 to 6 April 2011 to estimate this to be 4 PBq of ^{137}Cs and 11 PBq of ^{131}I. Tsumune et al. [T24] adjusted the release of ^{137}Cs in their model so that their estimate of average concentration between 26 March and 6 April fitted the average concentration measured at the southern outlet of FDNPS. This method resulted in a source term estimate of 3.5 ± 0.7 PBq of ^{137}Cs. The modelling work of Dietze and Kriest [D3] supported a source term in the range 1-4 PBq, rather than the much higher estimate reported in Bailly du Bois et al. [B2]; according to the analysis of Diest and Kriest [D3], the methodology used by Bailly du Bois et al. [B2] produced estimates of early releases (to mid-April) which were biased high and later releases (mid-April to July) which were biased low, and therefore total estimates from extrapolating backwards in time would be too high. Estournel et al. [E4] used a model with a relatively high resolution near the FDNPS site (600 m). The release of ^{137}Cs was calculated daily using an inverse method, constrained by

fitting to the observed concentrations at the two outlets of the plant. The total ^{137}Cs release to the ocean was estimated to be around 4.1–4.5 PBq. Estournel et al. adjusted this to a maximum value of 5.5 PBq to account for the observed increase in concentration 30 km offshore in mid-April, which had not been reproduced by the dispersion model (see section IV below). Charette et al. [C4] extrapolated the inventory of ^{134}Cs in the ocean from June 2011 back to early April, the period of the peak release. They thus estimated a value of 11 PBq for the direct release of ^{134}Cs, and that of ^{137}Cs could be assumed to be the same.

B28. Both Kawamura et al. [K3] and Estournel et al. [E4] estimated the time distribution of the releases to the ocean, and both showed a similar pattern that indicated direct releases to the ocean dominated over inputs from deposition of radionuclides released to atmosphere from around the end of March 2011 onwards. The release rates of ^{137}Cs as estimated by Estournel et al. [E4] are shown in figure B-V; they estimated that about 99% of the total direct release to ocean occurred before 22 April 2011. Measurements of radionuclide concentrations in seawater were not available before 21 March. The estimations by Estournel et al. for the period 11 March to 30 June assumed that concentrations in seawater before 21/23 March were the same as the first measured values.

Figure B-V. Estimated daily release of ^{137}Cs into the ocean [E4]

(Red: deposition from the atmosphere on to the ocean surface integrated over the whole modelling domain; blue: direct release calculated by inverse method)

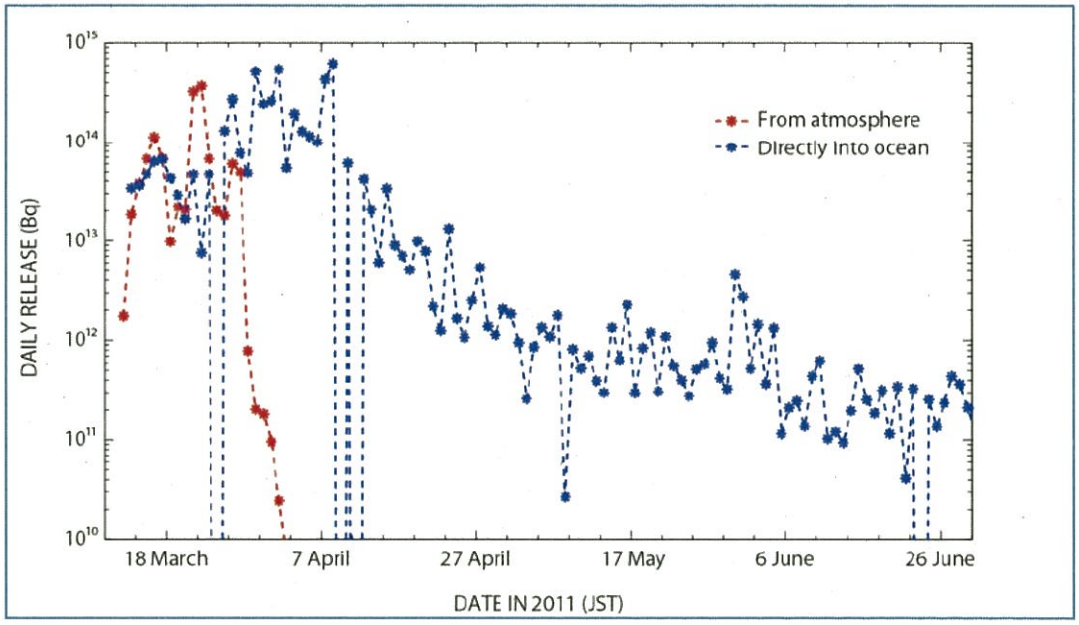

B29. Other radionuclides were also released to the ocean, both directly and indirectly. Isotopes of strontium and plutonium have been measured in seawater and sediments. Povinec et al. [P12] studied the measurements of concentrations of ^{89}Sr and ^{90}Sr in seawater. These generally showed strontium concentrations during the main period of the direct release to be one to two orders of magnitude lower than those of caesium. There was an exception to this general pattern around December 2011, when, following an accidental leakage of treated water from which caesium had been removed, measured concentrations of ^{89}Sr and ^{90}Sr, but not ^{137}Cs, rose [P12]. The concentrations of ^{90}Sr had fallen below those of ^{137}Cs again by January 2012. On the basis of different assumptions about the ratios of ^{90}Sr to ^{137}Cs and the range of estimates of total direct release of ^{137}Cs to the ocean, Povinec et al. estimated a

direct release of ^{90}Sr of between 0.04 PBq and 6.5 PBq (although the latter was based on the high estimated release of ^{137}Cs of 27 PBq by Bailly du Bois et al. [B2]).

B30. All of the estimates of releases to the ocean were associated with much uncertainty. In reviewing these estimates, the Committee gave more weight to results based on three-dimensional modelling taking into account the high variability of the dispersion, rather than to those derived with extrapolation methods using constant dispersion rates. It concluded that the direct release to the ocean of ^{137}Cs was likely to have been in the range of about 3–6 PBq, with the direct release of ^{131}I likely to be about three times higher. The direct release of ^{90}Sr could be estimated to be in the range of about 0.04–1 PBq (based on ratios to the ^{137}Cs release). The estimated direct releases of ^{137}Cs (about 3-6 PBq) were of a similar order of magnitude to the estimated deposition on to the ocean from releases to the atmosphere (about 5–8 PBq). For ^{131}I, deposition on to the ocean from releases to atmosphere (about 60–100 PBq) was estimated to be about 5–10 times higher than the direct releases. However, because the inputs from deposition on to the ocean surface provided a diffuse source, whereas the direct releases were from a localized source, direct releases accounted for most of the observed elevated concentrations in seawater around FDNPS from 26 March onwards. The dispersion of radionuclides deposited from the atmosphere and released directly to the ocean is considered further in section IV below.

III. TRANSPORT AND DISPERSION IN THE ATMOSPHERE

A. Meteorological conditions

B31. The meteorological conditions observed during the key episodes in the release of radioactive material to the atmosphere have been described by many authors [K15, K20, M25, S11, S12, W16]. From 9 to 11 March 2011, a weak low pressure trough over eastern Japan caused the appearance of light rain until 12 March in the morning (JST). Then, a high pressure system moved eastward along the south coast of the main island from 12 to 13 March; the wind direction was from the south below 1 km, and from the west above 1 km in altitude in the afternoon of 12 March, at the time when the hydrogen explosion occurred in Unit 1. During the period 14 to 15 March, another weak low pressure trough moved eastward off the southern coast of the main island, then moved toward the north-east while developing rapidly after 15 March. Some light rain was observed from 15 to 17 March in the morning because of a weak low pressure system that moved north-eastward off the east coast. In particular, rain was observed in Fukushima Prefecture during the night, from 15 March at 17:00 to 16 March at 04:00 [K15], a time corresponding with significant releases of radioactive material to the atmosphere. The low-level winds were from the south-west during the morning of 14 March, the time when a hydrogen explosion occurred at Unit 3. The 950 hPa winds were from the west until 14 March, but changed to a direction from north-north-east in the morning of 15 March, the time when significant releases occurred from Unit 2. During the period 18 to 19 March, a high pressure system dominated and winds were generally blowing from the west. A low pressure system was then observed passing over the main island from 20 to 22 March with moderate rain until 23 March in the Kanto area (Ibaraki, Chiba, Tochigi, Saitama and in Tokyo).

B. Synthesis of observations

B32. Dose-rate measurements provided a useful basis for estimating the source term by inverse or reverse modelling (see section II.A above); furthermore, they provided a valuable basis for assessing the quality of estimates made by atmospheric transport models of the dispersion of released material. Most of the measured dose rates came from portable monitoring posts deployed by Fukushima Prefecture during the accident. This was because many of the automatic monitoring posts in the prefecture did not operate during much of the period when the largest release occurred because of damage caused by the earthquake and tsunami. MEXT also published extensive dose-rate measurements made in each prefecture [N18], and particularly in Fukushima Prefecture.

B33. There were also some automatic stations recording dose rates continuously during the course of the accident. The spatial distribution of dose-rate stations in the vicinity of FDNPS is shown in figure B-VI.

Figure B-VI. Spatial distribution of dose-rate stations in the vicinity of FDNPS [F5]

B34. Dose-rate measurements made at three locations, namely Fukushima, Minamisoma and Kitaibaraki, are shown in figure B-VII.

Figure B-VII. Dose-rate measurements at Fukushima, Minamisoma and Kitaibaraki [F4, I8]

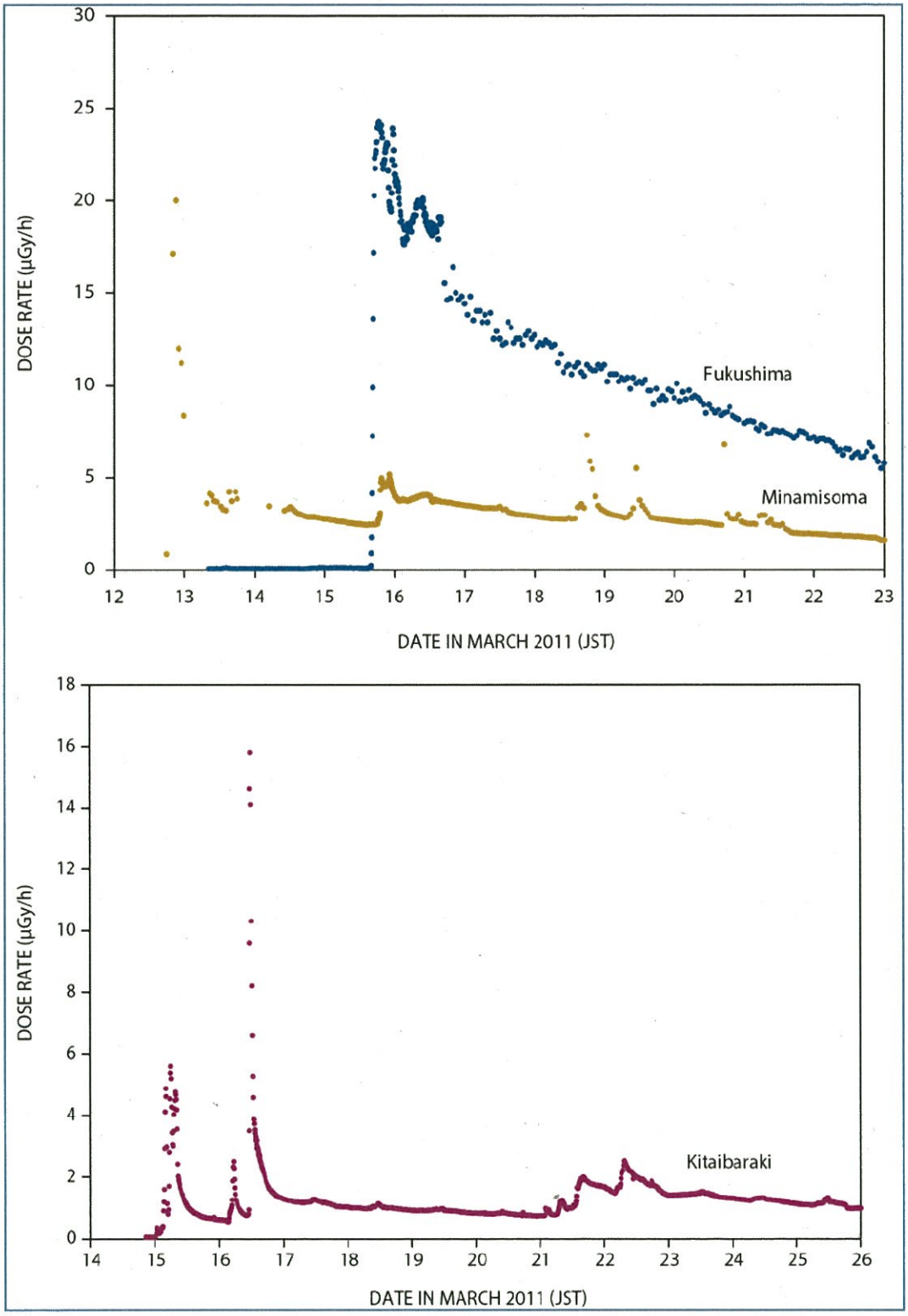

B35. In comparison, very few extended or continuous measurements in Japan were made, or have been published, of the concentration of radionuclides in air during the release period[33]. The few measurements of particular interest, because they spanned the whole period of major releases, comprised the following:

- Tokyo–Setagaya, located 250 km south-south-west of FDNPS;
- Tsukuba (Ibaraki Prefecture), located about 170 km from FDNPS in the direction of Tokyo;
- Takasaki (Gunma Prefecture) located 250 km south-west of FDNPS;
- Tokai-mura (JAEA office) located 100 km south-south-west of FDNPS.

The monitoring stations at Tokyo, Tsukuba, Takasaki and Tokai-mura were, however, all located in the Kanto area; consequently, their measurements were largely redundant; the exception is Takasaki where measurements were also made of the concentrations in air of noble gases.

B36. However, numerous and extensive measurements of the deposition densities of radionuclides were made. The United States Department of Energy measured deposition densities from aerial monitoring with fixed-wing aircraft from 17 March 2011 [U17] and ground measurements (in situ gamma spectrometry). MEXT subsequently, from June 2011, carried out a major campaign of aerial (helicopter) and ground measurements to cover the whole of the affected territory [N18]. The deposition density of ^{137}Cs on the ground surface is shown in figure B-VIII [N18].

[33] Outside of Japan, numerous measurements were made of concentrations of radionuclides in air when the released material passed overhead; these were used by many countries to assess doses to the public (see appendix C).

Figure B-VIII. Measurement results of the airborne monitoring surveys conducted by MEXT (deposition density of ^{137}Cs) [N18]

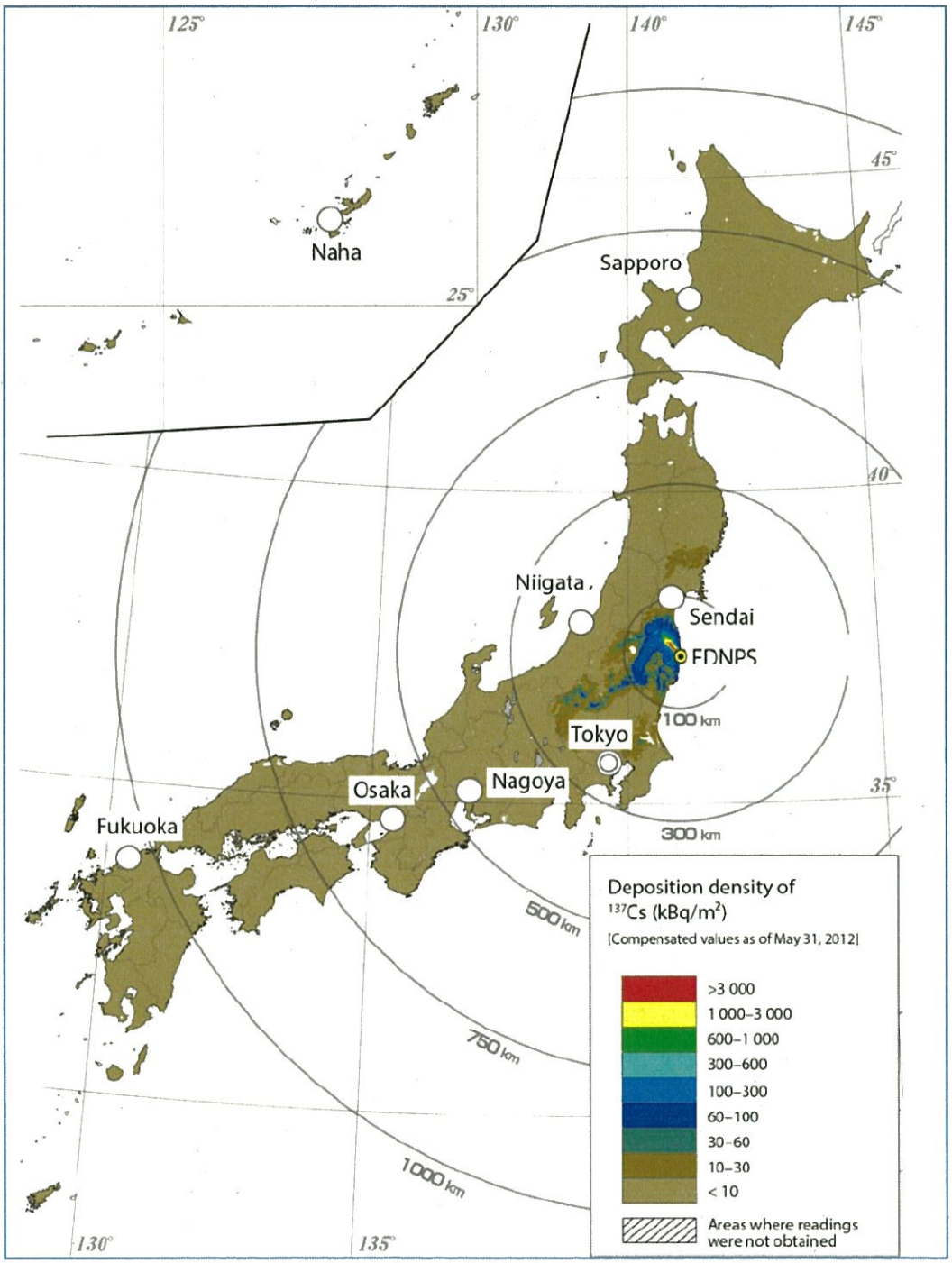

C. Atmospheric dispersion pattern

B37. Several events during the course of the accident led to major releases of radionuclides to the atmosphere (see table B1). Four periods were of particular interest in this respect.

B38. Venting and the hydrogen explosions in Units 1 and 3, during the period 12 to 14 March, were the origins of the initial and substantive releases of radioactive material to the atmosphere. The material released from Unit 1 spread mainly northwards along the eastern coast of the main island, then towards the north-east and east over the Pacific Ocean. This release was only detected by the Minamisoma station (see figure B-VI), located on the coast, about 25 km from FDNPS. No rainfall was recorded during this release episode. An increase in the dose rate during the night of 12 March was evident at the Minamisoma station (see figure B-VII) followed by a rapid decrease; this was characteristic of the passage of a radioactive plume in dry conditions. Simulations from one of the ATDMs used by a task team of the World Meteorological Organization (WMO) (see next section) of the ^{131}I concentration in air on 12 and 13 March, following the releases from Unit 1 and then Unit 3, are illustrated in figure B-IX. Owing to westerly winds, this plume travelled mostly towards the Pacific Ocean and had limited impact on the Japanese land mass.

B39. The material released from Unit 2 over the period 15 to 16 March was mainly due to the melting of the core and a breach of the reactor containment; this material was dispersed over eastern Japan because of rapidly changing weather conditions. This release episode could be better characterized than many others because it was monitored by many stations. It was the major contributor to the deposition of radioactive material on the Japanese land mass. The release took place in two quite distinct periods: firstly, during the night of 14 to 15 March; and, secondly, in the late morning and early afternoon of 15 March. From 00:00 to 05:00 JST on 15 March, the released material moved towards the south without encountering rain. An increase in the dose rate during the morning of 15 March was evident at the Kitaibaraki monitoring station (see figure B-VII). Radioactive material continued to be released throughout the rest of the day; this material moved towards the south then progressively towards the north-west and then to the south again on 16 March; these changes were reflected in the dose rates measured at the Kitaibaraki monitoring station (see figure B-VII) where two increases in the dose rate were recorded during 16 March. After 17:00 on 15 March, rainfall occurred until early morning of 16 March and this resulted in major deposition of radioactive material onto the ground; this was reflected in the large increase in the dose rate observed during the evening of 15 March at Fukushima (see figure B-VII). The relatively slow decrease in the dose rate at Fukushima is characteristic of radioactive material passing over a monitoring station in wet conditions (i.e. rainfall); the radionuclides deposited onto the ground by rain contribute to the dose rates measured by the monitoring station. Figure B-X shows simulations of the ^{131}I concentration in air at two times following the major releases that occurred from Unit 2; the simulated concentrations also include contributions due to continuing releases from Units 1 and 3.

B40. From the afternoon of 16 March onwards, subsequent releases, mainly from Units 2 and 3, spread easterly over the Pacific Ocean without any major impact for the Japanese territory. The simulated ^{131}I concentration in air during these releases is shown in figure B-XI.

B41. During the period from 20 to 23 March, releases from the three units were dispersed over the Japanese territory encountering rainfall on occasions. The simulated ^{131}I concentrations in air at particular times following these further releases from Units 1–3 are shown in figure B-XII.

B42. From 23 March, the release rates fell significantly and, compared with earlier releases, had minimal impact on the Japanese territory. The chronological patterns of atmospheric dispersion are seen as animations in attachments B-2 to B-3.

Figure B-IX. Simulated ^{131}I concentration in air during the initial releases from Units 1 and 3

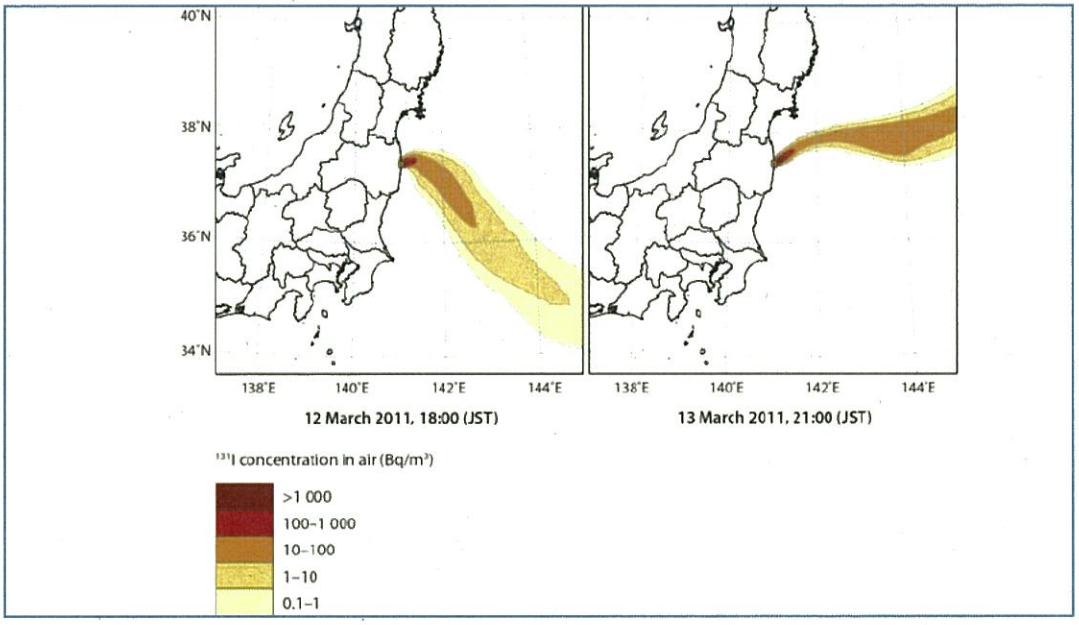

Figure B-X. Simulated ^{131}I concentration in air following the major releases from Unit 2 to the atmosphere

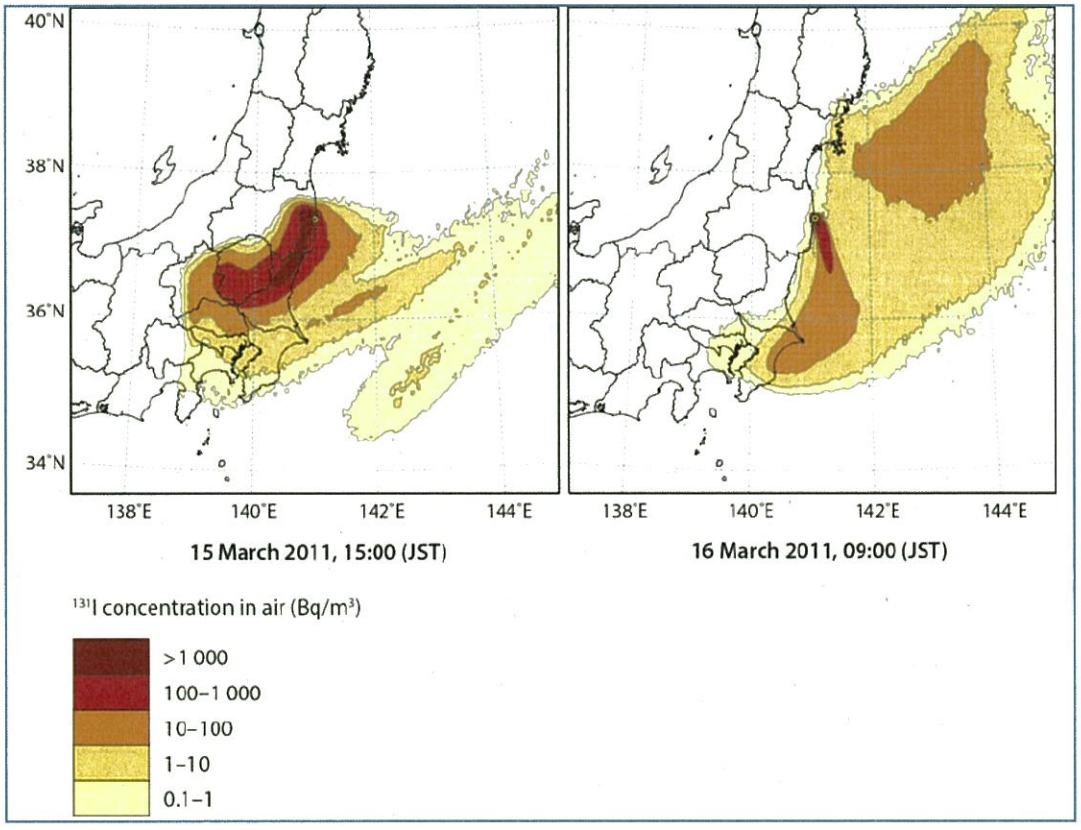

Figure B-XI. Simulated air concentration of ^{131}I during subsequent releases from FDNPS

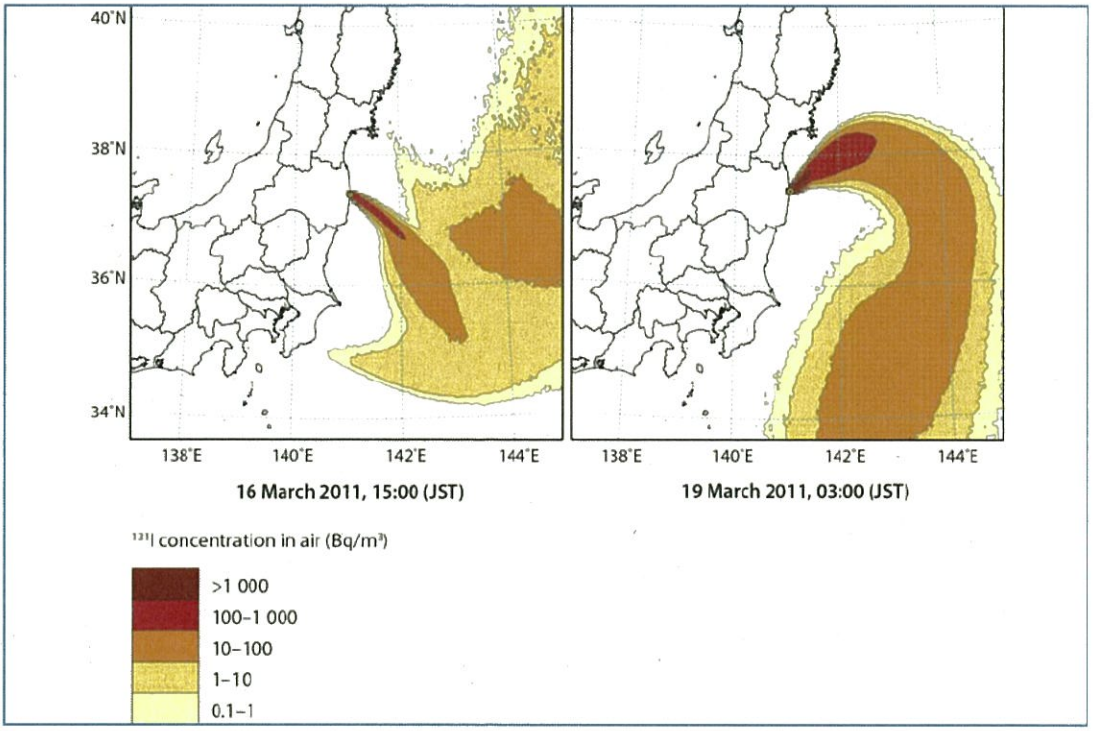

Figure B-XII. Simulated ^{131}I concentration in air during the releases from FDNPS in the period 20 to 23 March

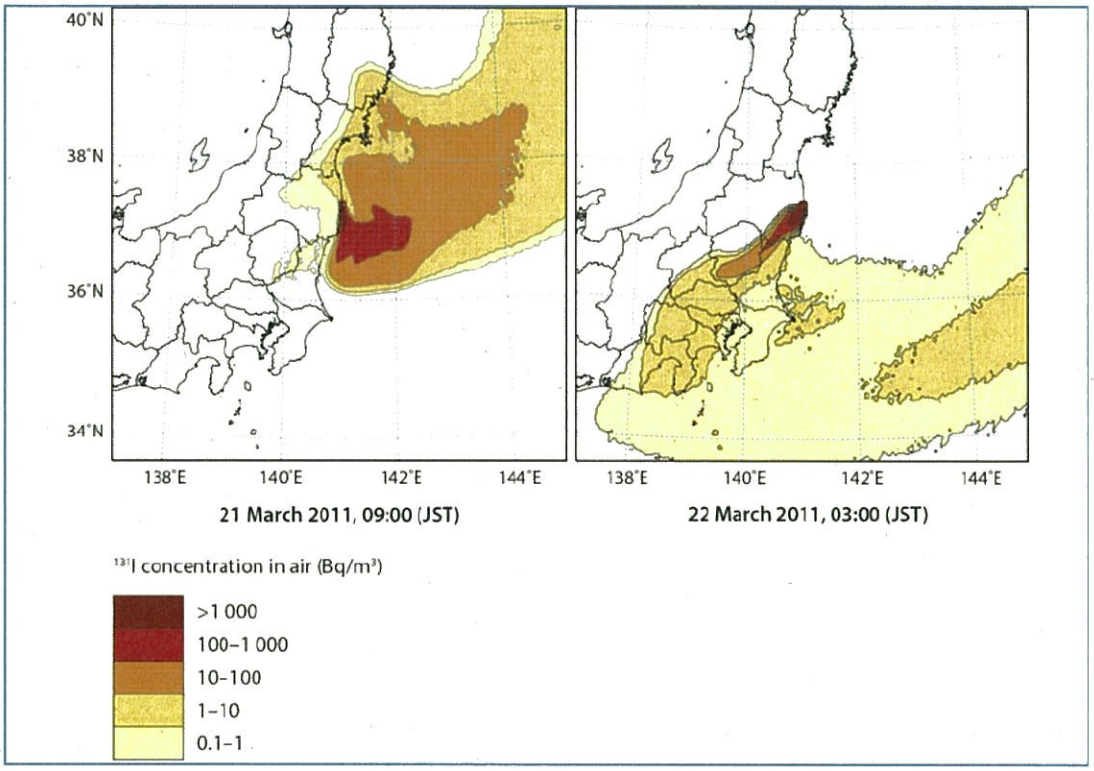

D. Methodology and results of dispersion and deposition assessment

B43. The World Meteorological Organization (WMO) organized a task team to advise the Committee on the use of meteorological analyses and data in estimating concentrations of released radionuclides in the terrestrial environment using atmospheric transport and dispersion models (ATDM). The task team approached this by applying the meteorological data to ATDMs and comparing the results with the available measurement data. The task team consisted of participants from the Canadian Meteorological Centre (CMC), the United States National Oceanic and Atmospheric Administration (NOAA), the United Kingdom Met Office (UKMET), the Japan Meteorological Agency (JMA), and the Austrian Zentralanstalt für Meteorologie und Geodynamik (ZAMG). Each of these participants used their institute's own models, each with its unique treatment of the meteorological input data, dispersion, and deposition computations. Each participant also used the computed fields derived from meteorological data analysis that were already available to them, as well as the higher spatial and temporal resolution fields provided by JMA. The results provided a range of solutions because of variations in model parameterizations and the meteorological analysis data. Further information on the meteorological analyses and the models can be found in the task team's final report [W18].

B44. Dispersion and deposition calculations for a unit source using each model–meteorology combination were made available on a website [N17] for three generic species of material: *(a)* a gas with no wet or dry scavenging (to represent noble gases such as ^{133}Xe); *(b)* a gas with a relatively large dry deposition velocity (0.01 m/s) and wet removal (to represent released iodine in a gaseous form); and *(c)* a particle with wet removal and a small dry deposition velocity (0.001 m/s) (to represent all other released radionuclides, including iodine in a particulate form). These could be used to estimate concentrations in air and deposition densities of radionuclides on the ground for any postulated source term subject to specifying the time dependence of release rates for each released radionuclide.

B45. In order to evaluate the performance of the various ATDM–meteorology combinations, the WMO task team used a provisional source term estimate that had been developed prior to the Committee making a formal choice on what to use for its dose assessment. The provisional source term differed in a number of respects from that finally adopted by the Committee, but was sufficiently similar not to prejudice the main findings relating to the performance of different ATDM–meteorology combinations[34]. The results for each ATDM–meteorology combination can be found in [W18] where they were compared with the measurements of deposition densities of radionuclides and the more limited measurements of concentrations in the air. The outcome of the evaluation was inconclusive with respect to which ATDM–meteorology combination provided the best fit to the measured deposition densities and concentrations of radionuclides in air: the best fit for deposition density was not the same as that for concentration in air. To obtain better fits, the mean of the ten most representative ATDM–meteorology combinations was computed and compared with the measurement data. Statistical analysis showed that this "ensemble mean" provided a better fit than any individual ATDM–meteorology combination for both deposition density and radionuclide concentration in air. The performance of some ATDM–meteorology combinations was, however, not dissimilar to that of the ensemble mean [W18].

B46. In estimating the dispersion and deposition of radioactive material released from FDNPS, a number of simplifying assumptions had to be made to configure the ATDM simulations. Most of these

[34] Since this work was completed, task team members carried out further analyses using the Terada et al. source term [T19] (that is the source term adopted by the Committee for its assessment). The performance of the various ATDM–meteorology combinations for this source can be found in [D4].

concerned the characteristics of the source term as estimated by Terada et al. [T19] and were made as a compromise to accommodate the following potentially conflicting demands: *(a)* faithfully representing the varying radionuclide release rates; *(b)* the spatial and temporal resolution of the available meteorological data; and *(c)* the computational time and storage requirements of the subsequent simulations made using the ATDM in the WMO work. The main simplifications were the following: *(a)* release rates were specified in three-hourly time intervals as opposed to the finer resolution given by Terada et al. [T19] for particular release periods; *(b)* all releases were assumed to occur from, and be uniformly distributed over, a column from the ground to a height of 100 m, rather than characterizing the specific events leading to the releases (for example, hydrogen explosions and venting).

B47. For the assessment of exposures in the non-evacuated areas, the ATDM results were used to estimate the concentrations of radionuclides in air from measured deposition densities on the ground by scaling the measured deposition densities by the ratio of the concentration in air and deposition density estimated by one or other ATDM–meteorology combination. Despite the better performance of the ensemble mean (in terms of estimating measured levels in the terrestrial environment), the use of a single ATDM was judged to be more appropriate for most of the Committee's purposes.

B48. Estimates of the "bulk deposition velocity" for ^{137}Cs at selected locations (that is the ratio of the deposition density to the time integral of concentration in air) are given in table B7 for five of the best performing ATDM–meteorology combinations of the ten combinations that constituted the ensemble mean. The values for a given location varied within a range of about three to ten but, typically, by about five. This variability provided an indication of the uncertainty associated with inferring concentrations in air (and thus internal exposures via inhalation) from measured deposition densities. In general, the contribution of inhalation to the total exposure from all pathways was small; consequently, variability of the magnitude indicated above was unlikely to have had much impact on the overall precision of estimated doses.

Table B7. Comparison of "bulk deposition velocities" for ^{137}Cs estimated by different ATDM–meteorology combinations for selected locations

Location/Model	*"Bulk deposition velocity" (mm/s) for ^{137}Cs[a]*					
	NOAA-GDAS[b]	*UKMET-MESO[c]*	*UKMET-ECMWF[d]*	*NOAA-ECMWF*	*ZAMG-ECMWF*	*Average*
Okuma Town[e]	6.2	3.3	3.2	3.4	1.2	3.4
Iwaki City	6.8	3.2	6.1	7.6	8.8	6.4
Fukushima City	91	160	71	66	340	140
Iitate Village[e]	48	52	250	200	130	140
Namie Town[e]	48	24	240	87	80	97

[a] *The bulk deposition velocity is the ratio of the estimated deposition density on the ground and the estimated integrated radionuclide concentration in air; it was used to infer integrated concentrations in air from deposition density measurements for estimating internal exposures from inhalation of radioactive material (see appendix C).*

[b] *GDAS – Global Data Assimilation System*

[c] *MESO – Mesoscale Analysis provided by the Japan Meteorological Agency (JMA).*

[d] *ECMWF – European Centre for Medium range Weather Forecasting.*

[e] *Bulk deposition velocities were not used for assessing exposures in evacuated areas (Okuma Town, Namie Town and Iitate Village were all evacuated).*

B49. Given this limited sensitivity, the choice of which ATDM–meteorology combination to use had limited practical significance for the Committee's assessment of doses. The Committee chose the NOAA-GDAS ATDM–meteorology combination for the purposes of estimating ratios; this model was one of the higher ranked combinations[35], indeed even more highly ranked than the ensemble mean for deposition of ^{137}Cs. Compared with the average ratios of the five combinations at particular locations, the use of the NOAA-GDAS combination led to inferred concentrations in air that were typically within a factor of two lower or higher.

B50. The ^{137}Cs deposition pattern computed by NOAA-GDAS (figure B-XIII) was compared with the measured deposition pattern. The modelling results reproduced the observed deposition pattern quite well. The NOAA-GDAS calculations of the concentrations in air were compared to measured concentrations in air at the JAEA sampling site [F7, O2] (figure B-XIV); the comparison was not as good, capturing only three of the four main peaks and estimating the size of the peaks only within about a factor of ten. While the modelling results were able to capture the general pattern of radionuclide concentrations in the environment spatially and temporally, their ability to reproduce deposition density or concentration in air accurately at any particular time or location may have had considerable uncertainty; this is illustrated in figure B-XV where the NOAA-GDAS predictions are compared with the corresponding measurement of ^{137}Cs deposition density. The predictions showed little bias compared to the measured deposition densities. However, the uncertainty for specific locations varied by more than a factor of ten for the lowest deposition densities, but fell with higher deposition densities; at the highest deposition densities, the model predictions underestimated those measured by a small factor.

B51. The results of the ATDM simulations were used in a different way for estimating the concentrations in air and deposition densities of radionuclides to which the early evacuees were exposed. No data were available on the measured deposition densities before or during the evacuations; consequently, the method for estimating concentrations of radionuclides in air from deposition density measurements and a ratio derived from ATDM simulations could not be used. Instead, the time-dependent radionuclide concentrations in air and deposition densities estimated by the ATDM simulations were used directly. For reasons of consistency with the estimation of radionuclide concentrations in air for non-evacuees from the measured deposition densities, the NOAA-GDAS combination was also used here for estimating concentrations in air (and deposition densities) to which the early evacuees were assumed to be exposed. Given the inherent uncertainties in the estimates of these models for any given location, the choice of the NOAA-GDAS combination (relative to any other ATDM–meteorology combination or an average of several) was unlikely to be of great practical significance (see section E).

[35] Ranked in terms of a complex statistical measure related to how well a model was able to replicate measured levels in the environment (see [W18]).

Figure B-XIII. The calculated ^{137}Cs deposition density using the NOAA-GDAS combination

The contours show the terrain elevation at 250 m intervals

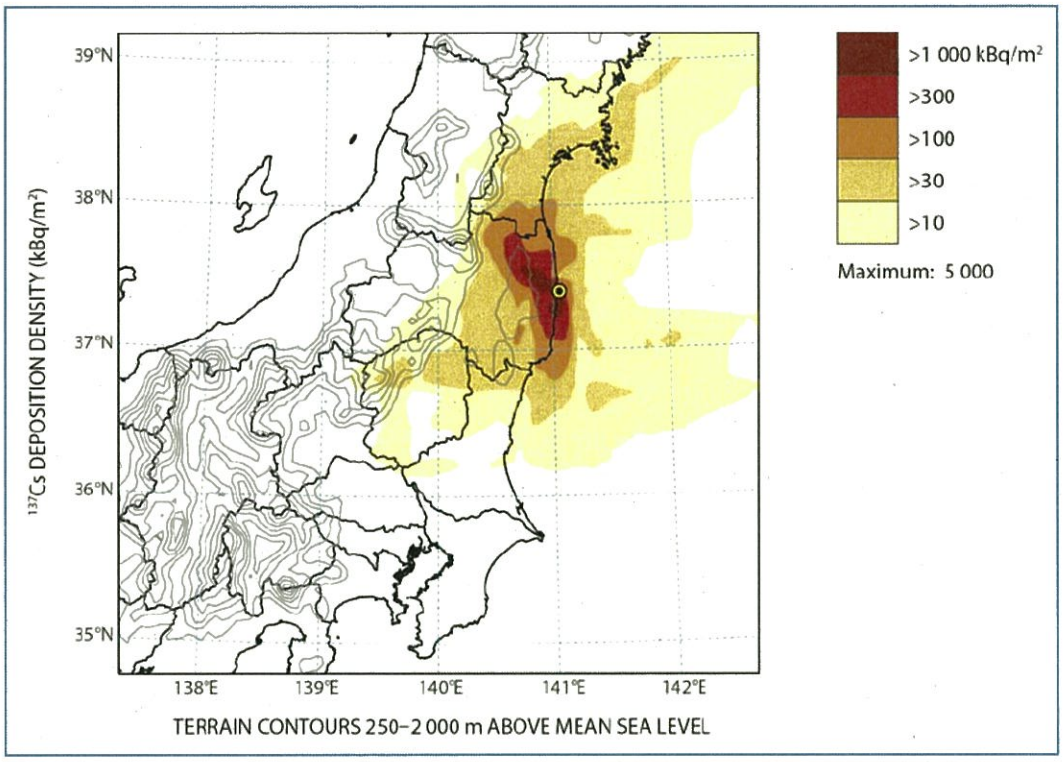

Figure B-XIV. The calculated ^{137}Cs concentrations in air (red +) using the NOAA-GDAS combination and measured data at Tokaimura, Ibaraki, Japan (black o) [F7, O2]

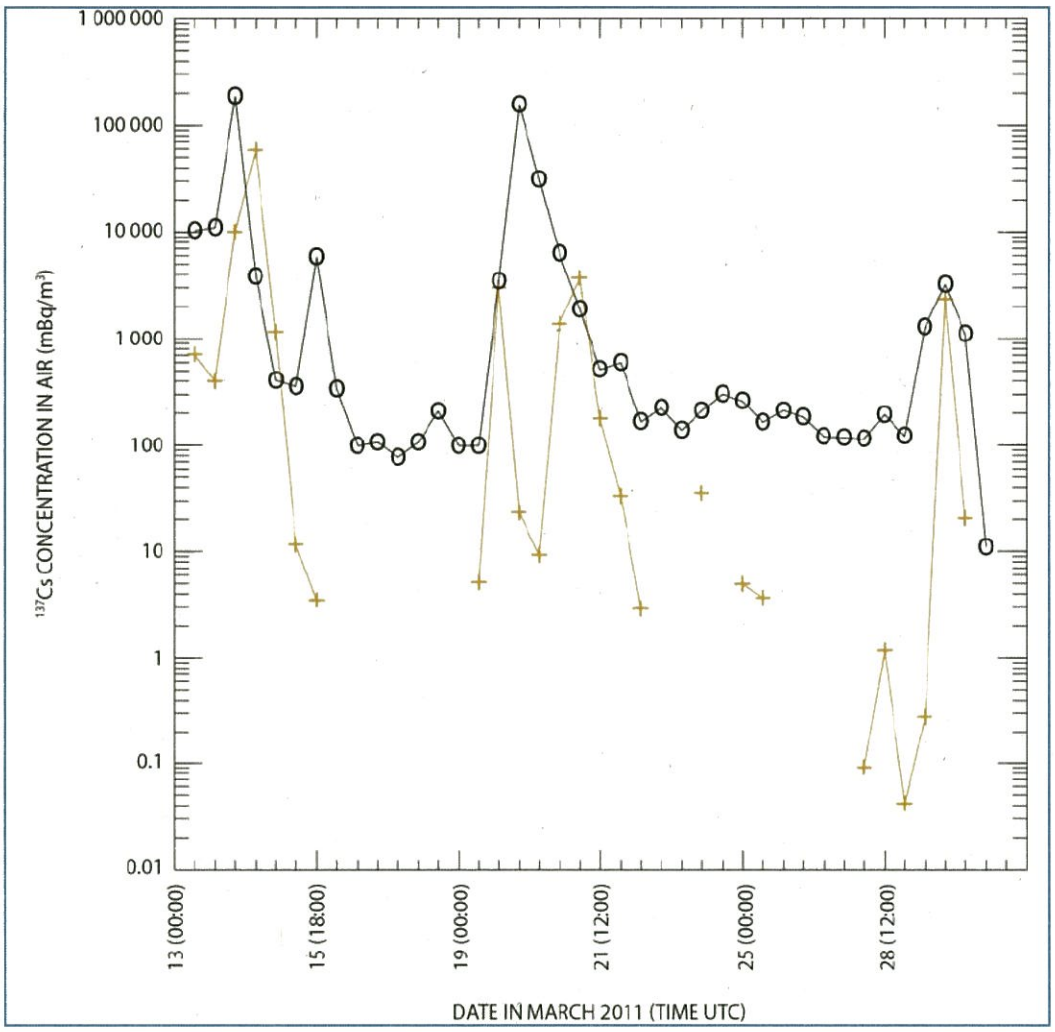

Figure B-XV. Scatter plot comparing NOAA-GDAS estimates and measurements of ^{137}Cs deposition density

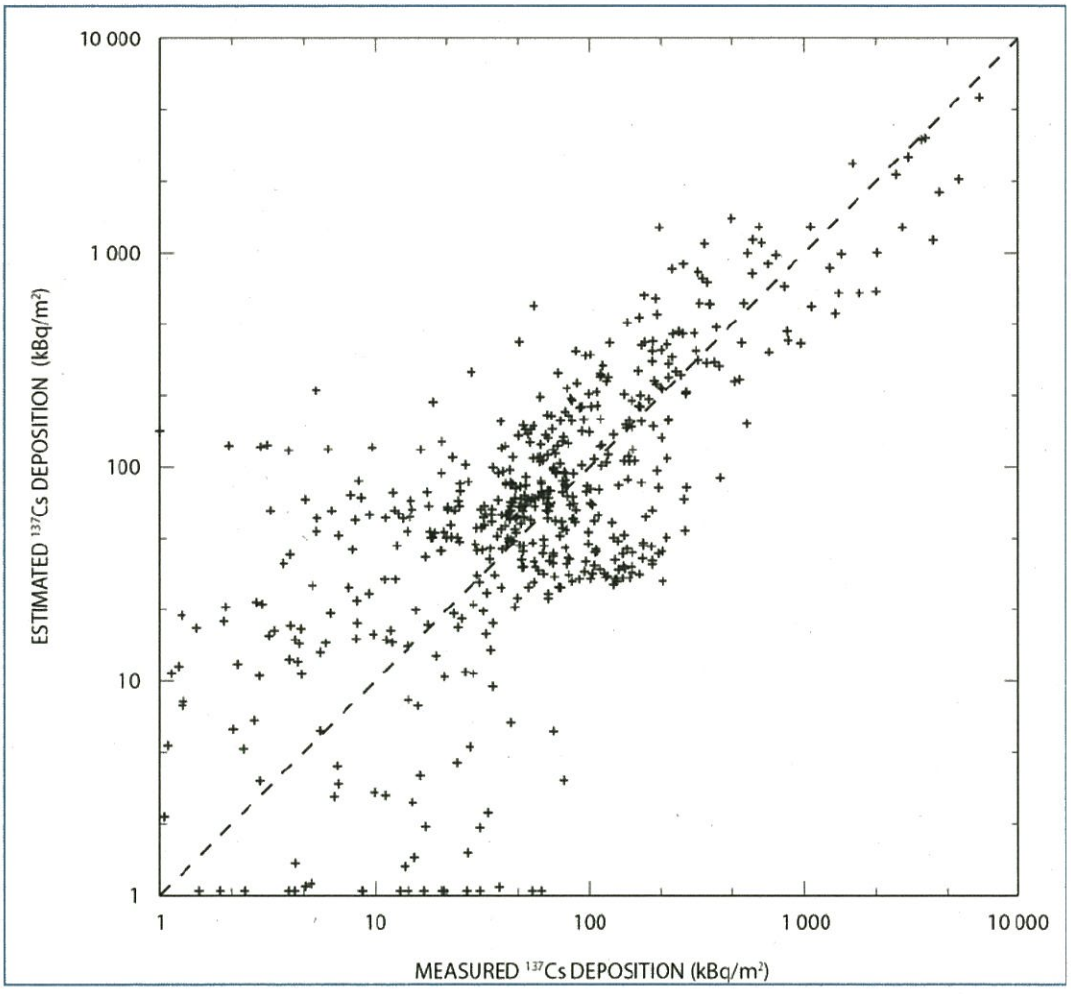

E. Robustness of estimation of radionuclide levels in the environment where no measurements are available

B52. The ATDM estimates of the concentrations of radionuclides in air and deposition densities on the ground were associated with much uncertainty resulting from uncertainties in the source term and how material was dispersed in and deposited from the atmosphere. A rigorous analysis of these uncertainties was beyond the scope of this assessment. However, indications of the robustness of the estimates made in this assessment were made by conducting more limited scoping studies.

B53. For this purpose, separate estimates were made, using an independently derived and applied source term–ATDM–meteorology combination (that was not part of the WMO group), of the main quantities used to calculate doses to people; these quantities were time integrals (total and truncated) of concentrations of radionuclides in air and their deposition density on the ground, and ratios of these two quantities used to infer concentrations in air from measured deposition densities.

B54. The NOAA-GDAS ATDM results were compared with an IRSN ATDM–meteorology combination, namely an IRSN–ECMWF model using the source term of Saunier et al. [S3], which was derived using a different methodological approach, and measurements that were largely independent from those used by Terada et al. [T19] (the source term adopted by the Committee). The main features of, or assumptions adopted in, the two source term–ATDM–meteorology combinations are summarized in table B8. A comparison of the two source terms is also provided in figure B-XVI, where the time-dependent releases of ^{131}I are shown. A comparison of the time-dependent releases of ^{137}Cs is given in figure B-I, at least for the first few days when the releases were largest. Much greater temporal resolution was apparent in the Saunier et al. source term estimate consequent upon it being derived from numerous measurements of dose rate that were, in general, continuous throughout the release period.

Table B8. Comparison of the main features and assumptions in the two source term–ATDM–meteorology combinations

Characteristics of the source term–ATDM–meteorology combinations		*Terada–NOAA-GDAS*	*Saunier–IRSN-ECMWF*
Source term	Basis of derivation	Reverse modelling of environmental measurements (concentrations in air, deposition densities, dust samples, dose rates) Total releases: ^{131}I, 120 PBq; ^{137}Cs, 8.8 PBq	Inverse modelling of generally continuous dose-rate measurements from 57 monitoring stations in Japan Total releases: ^{131}I, 103 PBq; ^{137}Cs, 16 PBq
	Release heights	Assumed spread uniformly over a column from ground to height 100 m	Assumed spread uniformly over a column from ground to height 160 m
	Form of release	All nuclides released as particulates apart from noble gases, and iodine (assumed half released as particulate and half as elemental gaseous iodine)	Apart from noble gases, all nuclides released as particulates
Meteorology	Source	NOAA global analysis [W18]	ECMWF [W18]
	Time resolution	3 hourly	Hourly
	Spatial resolution	0.5° latitude and longitude	0.125° latitude and longitude
	Vertical resolution	56 layers; 10 within the lowest 1 km	11 layers between 0 and 3 400 m
Atmospheric dispersion and deposition	ATDM model	HYSPLIT [D5]	IdX [S3]
	Dry deposition	Particulates 10^{-3} m/s Elemental iodine 10^{-2} m/s	Particulates 2×10^{-3} m/s
	Wet deposition	Particulates in-cloud 4×10^{4} L/L Particulates below-cloud 5×10^{-6} s^{-1} Gaseous iodine 0.08 M/a solubility [D6]	$5 \times 10^{-5} p_0$ where p_0 is the precipitation rate (mm/h)

Figure B-XVI. Comparison of the time-dependent releases of ^{131}I estimated by Terada et al. [T19] and Saunier et al. [S3]

(a) Period of 12 to 17 March 2011

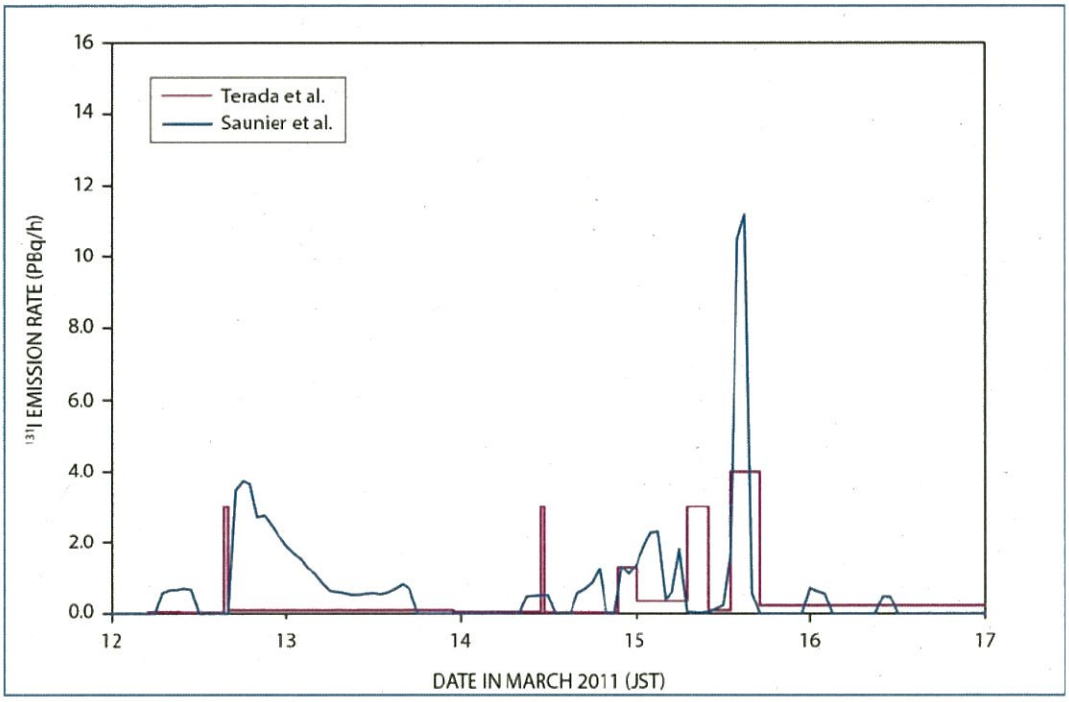

(b) Period 17 to 27 March 2011 (Note: different vertical scale to that used in (a))

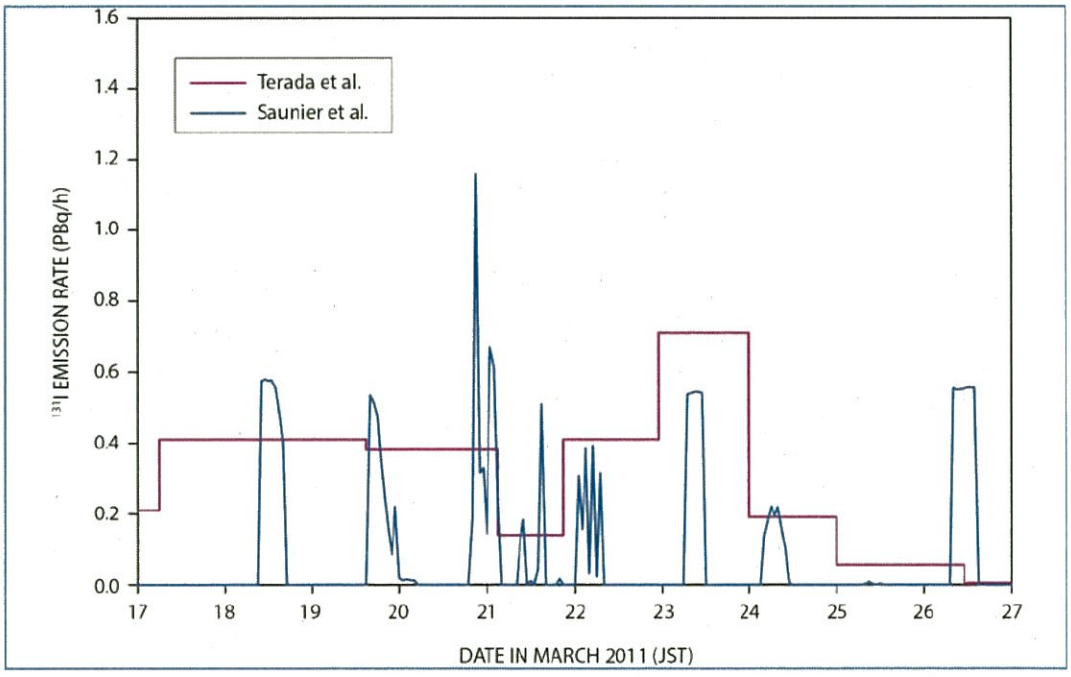

B55. Table B9 shows the "bulk deposition velocities" estimated by the Terada–NOAA-GDAS combination and the Saunier–IRSN-ECMWF combination (referred to as "NOAA" and "IRSN" in the table) at selected locations for ^{131}I and ^{137}Cs. In addition, the ratio of the IRSN and NOAA ratios are also shown to indicate by how much the estimated concentrations in air (and thus the doses from inhalation) would have been different had the IRSN combination been used instead of the NOAA combination.

Table B9. Comparison of "bulk deposition velocities" for ^{131}I and ^{137}Cs estimated by different source term–ATDM–meteorology combinations for selected locations

Location/Model	^{131}I			^{137}Cs		
	NOAA (mm/s)	IRSN (mm/s)	Ratio IRSN to NOAA	NOAA (mm/s)	IRSN (mm/s)	Ratio IRSN to NOAA
DELIBERATE EVACUATION AREA						
Iitate Village	28	42	1.5	48	28	0.58
NON-EVACUATED LOCATIONS						
Iwaki City	8.5	5.6	0.65	6.8	4.9	0.71
Fukushima City	34	150	4.4	91	95	1.1

Note: The bulk deposition velocity is the ratio of radionuclide deposition density to the integrated concentration in air used to infer concentrations in air from measured deposition densities on the ground and thus estimate internal exposure from inhalation of radioactive material.

B56. For ^{137}Cs, the bulk deposition velocities estimated by the IRSN combination were, on average, about 20% lower than those estimated by the NOAA; at specific locations, they ranged from about 10% higher to a factor of about 1.5 lower, depending on the location. For the same value of measured deposition density, these differences would have translated into inferred concentrations in air (and thus doses from inhalation for the non-evacuated areas) ranging from about 10% lower to about a factor of 1.5 higher, depending on the location, compared with those estimated by the Committee using the NOAA combination.

B57. For ^{131}I, the bulk deposition velocities estimated by the IRSN combination ranged from about a factor of about 4 higher to a factor of about 30% lower—depending on the location—than those estimated by NOAA. These differences would have translated into inferred concentrations in air (and thus doses due to inhalation for the non-evacuated areas) ranging from about a factor of 30% higher to about a factor of 4 lower, depending on the location; on average, they would have been about 40% lower compared with those estimated by the Committee using the NOAA combination.

B58. The time integrals (truncated to when evacuation occurred) of the concentrations of ^{131}I in air and deposition densities estimated by the NOAA and the IRSN combinations are shown in table B10 at 14 selected locations and times relevant to the estimation of doses to early evacuees. The ratios of truncated concentrations in air estimated by the IRSN and NOAA combinations (and likewise the ratios of their respective estimates of deposition densities) are also shown in the table; the variation in these ratios was much greater than in the ratios of the two quantities (i.e. ratios of concentration in air and deposition density, see table B9).

B59. For 9 of the 14 locations, the IRSN estimates for ^{131}I concentration in air were within a factor of two of those for NOAA, and, for most locations, the ratios varied between about 0.5 and 12 (ignoring the value of zero for Futaba Town and 2,100 for Minamisoma City). For deposition, the IRSN estimates

were within a factor of two of those for NOAA for 6 out of 14 locations, and for most locations (13 out of 14) the ratios varied between about 0.2 and 8 (ignoring the value of zero for Futaba Town). This level of variability was not unexpected and was typical of the uncertainty associated with the use of ATDM–meteorology combinations to estimate concentrations in air and deposition densities at specific locations; this variability was further compounded by the use of different source terms in the two cases. The implications of this variability for the estimation of doses to evacuees are further addressed in appendix C.

Table B10. Comparison of the time-integrated concentration of ^{131}I in air and deposition density estimated by two combinations of source term, ATDM and meteorology

Location	*Time period*		*NOAA*		*IRSN*		*Ratios (IRSN/NOAA)*	
	From	*To*	*Time-integrated concentration in air (Bq s/m³)*	*Deposition density (Bq/m²)*	*Time-integrated concentration in air (Bq s/m³)*	*Deposition density (Bq/m²)*	*Time-integrated concentration in air*	*Deposition density*
Kawauchi Village	2011-03-12 11:00	2011-03-16 08:00	3.4×10^{7}	4.1×10^{5}	4.0×10^{8}	2.9×10^{6}	11	7.0
Okuma Town	2011-03-11 21:23	2011-03-12 04:00	0	0	0	0	1	1
Kawamata elementary school	2011-03-12 08:00	2011-03-19 08:00	6.8×10^{7}	2.2×10^{6}	7.5×10^{7}	2.7×10^{6}	1.1	1.2
Futaba Town	2011-03-11 21:23	2011-03-12 21:00	8.4×10^{7}	5.6×10^{5}	0	0	0	0
Kawamata elementary school	2011-03-12 21:00	2011-03-19 17:00	6.8×10^{7}	2.2×10^{6}	7.5×10^{7}	2.7×10^{6}	1.1	1.2
Iwaki City	2011-03-12 13:00	2011-03-31 12:00	2.9×10^{8}	2.5×10^{6}	1.5×10^{8}	8.1×10^{5}	0.51	0.33
Iwaki City	2011-03-12 13:00	2011-03-16 15:00	2.2×10^{8}	1.2×10^{6}	1.1×10^{8}	2.5×10^{5}	0.50	0.21
Namie Town Tsushima activation centre	2011-03-12 15:00	2011-03-16 10:00	2.2×10^{8}	6.8×10^{6}	1.7×10^{8}	3.1×10^{6}	0.75	0.46
Tamura City, Denso Higashinihon	2011-03-12 08:00	2011-03-31 08:00	9.4×10^{6}	3.6×10^{5}	9.4×10^{7}	2.5×10^{6}	10	6.9
Minamisoma City	2011-03-11 00:00	2011-03-15 10:00	1.3×10^{5}	9.3×10^{5}	2.7×10^{8}	5.7×10^{5}	2100	0.61
Date City office	2011-03-15 16:00	2011-03-31 11:00	1.8×10^{7}	3.1×10^{5}	1.9×10^{7}	2.1×10^{6}	1.1	6.8
Kawauchi Mura elementary school	2011-03-13 11:00	2011-03-16 10:00	3.3×10^{7}	4.0×10^{5}	3.9×10^{8}	3.1×10^{6}	12	7.9
Namie Town Tsushima activation centre	2011-03-11 00:00	2011-03-23 14:00	2.8×10^{8}	7.4×10^{6}	1.8×10^{8}	3.9×10^{6}	0.64	0.53
Katsurao Village	2011-03-11 00:00	2011-03-21 12:00	2.4×10^{8}	5.5×10^{6}	2.4×10^{8}	4.0×10^{6}	0.99	0.74

IV. TRANSPORT AND DISPERSION IN THE OCEAN

A. Synthesis of observations

(a) *In the water column*

B60. Numerous observations of radionuclides were made in the northern Pacific Ocean over a wide range of distances from FDNPS, beginning one week after the accident [B25, H7, M11, T6]. Measurements were also made in the Sea of Japan to assess the radionuclide concentrations on the western side of the archipelago. These data provided a relatively good understanding of the spatial and temporal distribution in the ocean of ^{137}Cs and ^{134}Cs, the most radiologically significant radionuclides released.

B61. Isotopes of other elements were also measured, including: ^{131}I, which was measured at elevated concentrations but only over a limited time because of its relatively short half-life of 8 days; ^{129}I, which was detected near the Japanese coast; and ^{89}Sr and ^{90}Sr, which were detected near FDNPS in 2011 and 2012 and, for ^{90}Sr, over a larger area (30 to 600 km) in June 2011.

(b) *Observations of ^{131}I, ^{134}Cs and ^{137}Cs*

B62. On 21 March 2011—within ten days of the first release of radionuclides from FDNPS—the operator, TEPCO, began to conduct monitoring of seawater near one of the two outlets located on either side of the FDNPS port [T6]. Monitoring was also carried out inside the port. Three days later, the monitoring was extended to the second outlet. Monitoring for ^{131}I, ^{134}Cs and ^{137}Cs was then conducted at points near each of these outlets twice daily. The results for ^{137}Cs in seawater near FDNPS are shown in figure B-XVII [B23]. They indicated that concentrations of ^{137}Cs increased to a first peak at 47,000 Bq/L on 31 March, followed by a second peak at 68,000 Bq/L on 7 April, before declining rapidly to under 10,000 Bq/L by 9 April and generally below 200 Bq/L by the end of April. Thereafter, the decrease was much slower. The ratio of the concentrations in seawater of ^{134}Cs to those of ^{137}Cs was found to be very close to 1. In 2012, concentrations of ^{137}Cs measured near the two outlets were between 1 and 10 Bq/L. Measurements of concentrations in the port during 2012 ranged between 10 and 100 Bq/L, indicating that some releases were continuing, possibly from residual leaks, from underground water sources, from run-off into rivers from deposits on land, or from desorption of radionuclides from marine sediments.

Figure B-XVII. Measured concentrations of ^{137}Cs in seawater near the FDNPS site [B23]

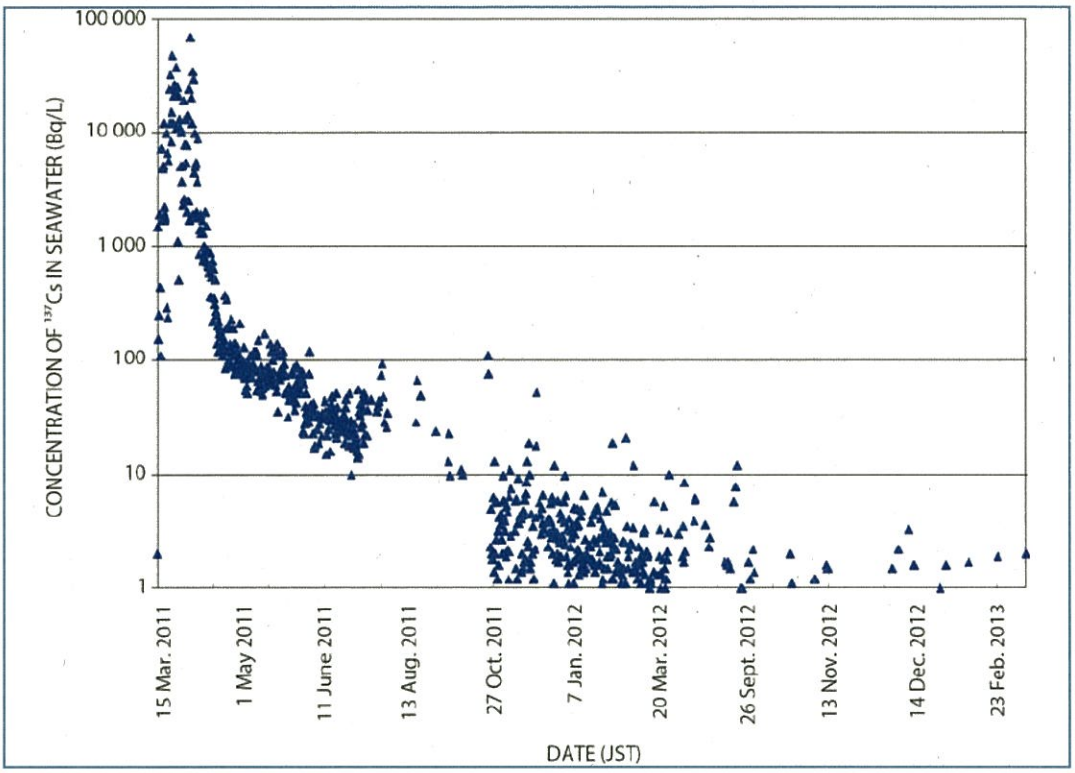

B63. During the first days of monitoring, concentrations of ^{131}I in seawater 20 to 30 times higher than of ^{137}Cs were measured, reflecting the relative importance of atmospheric deposition at this time. Around 25 March, the ratio of the two radionuclides in the vicinity of FDNPS fell sharply to 10. By around mid-May, this ratio was close to 0.1, reflecting the comparatively short half-life of ^{131}I.

B64. TEPCO also conducted monitoring in coastal waters further away from FDNPS [T6], and increased the number of measurement stations over time. Two coastal stations south of FDNPS were monitored daily: the first 11 km to the south at the Fukushima Daini Nuclear Power Station; and the second 16 km to the south at Iwasawa beach. TEPCO progressively added other sites, both along the coast and on sections located 3 km, 8 km and 15 km offshore. In addition, MEXT [M11] performed regular measurements at different stations on a section located 30 km from the coast.

B65. During the period characterized by large direct liquid releases (between 26 March and 8 April), dispersion of the released radionuclides away from FDNPS was relatively limited. Concentrations at the monitoring site 11 km to the south, where they were the next highest after the FDNPS outlets, were approximately 20 times lower [T6]. Moreover, concentrations fell even more rapidly with distance over this period perpendicular to the shoreline. At 15 km offshore, concentrations were 100 times lower than at FDNPS and, at 30 km offshore, they were about 1,000 times smaller. After 8 April, when the concentrations measured in seawater at FDNPS peaked, concentrations at 30 km offshore increased significantly for a few days suggesting a mechanism of seaward dispersion. From the middle of May, samples collected 15 km offshore by TEPCO were most often below the relevant detection limit.

B66. Regarding the dispersion along the coast, a comparison of two sites to the north and to the south located at the same distance from FDNPS [T6] indicated that the coast south of FDNPS would have

been more affected than the northern coast. However, this indication should be treated with caution because the northern coast was not monitored during the period of large direct releases.

B67. Various scientific cruises were made at distances farther from FDNPS between April and June 2011 [B25, H7]. In addition, ships voluntarily took measurements across the entire northern Pacific Ocean at least up until March 2012 [A12]. The detection limits for these measurements were lower than those of the regular monitoring discussed above.

B68. One month after the accident, a scientific cruise aimed at measuring ^{134}Cs and ^{137}Cs was organized several hundred kilometres from the Japanese coast with an additional extension to about 2,000 km towards the north-east [H7]. The concentrations of ^{137}Cs were found at up to 100 times higher than the pre-accident levels. The ratio of these two caesium radionuclides was found to be close to one, indicating that the source was FDNPS. The presence of these radionuclides in the north-east and south-east directions at such a large distance from FDNPS so shortly after the accident indicated that their presence was mainly because of atmospheric inputs.

B69. In June 2011, a cruise conducted measurements with a relatively high spatial density between 30 and 600 km from the Japanese coast of radionuclide concentrations in the surface and subsurface waters [B25]. The concentrations of ^{134}Cs were highest near the coast. At 600 km offshore, concentrations at the surface reached 0.1–0.3 Bq/L. A clear finding of this sampling work was that the concentrations to the south of the Kuroshio current were low, showing that this powerful current formed a southern boundary for liquid releases from FDNPS.

B70. Finally, for the period from March 2011 to March 2012, other ships sampled the northern Pacific Ocean between 20°N and 50°N [A12]. The results showed radiocaesium was moving towards the east at a rate close to 80 mm/s. The main body of the radioactive plume reached longitude 180°E (more than 3,000 km from the station) in March 2012, one year after the accident, with a maximum concentration of 10^{-2} Bq/L. This propagation was confined along the parallel of 40°N latitude.

B71. Generally, measurements where the detection limit was high (10 to 20 Bq/L) did not detect released radionuclides in seawater below the surface. More precise measurements with a lower detection limit indicated that ^{134}Cs concentrations decreased significantly with depth below the ocean surface. In June 2011, released radiocaesium in a dissolved form apparently had not penetrated below 100–200 m from the ocean surface [B25].

(c) *Other radionuclides*

B72. Radiostrontium (^{89}Sr and ^{90}Sr) was detected in measurements made regularly over a year at FDNPS [P12] and offshore during a cruise in June 2011 [C2]. At FDNPS, ^{90}Sr concentrations were up to 4 orders of magnitude higher than those that preceded the accident, but were generally at least one order of magnitude lower than those of ^{137}Cs (except for the short period following the direct release to the ocean in December 2011—see section II.B above). Further offshore, in June 2011, the ratio of the concentration of ^{90}Sr in seawater to that of ^{137}Cs was about 0.02. This concentration ratio was much higher in seawater than in ground deposition, indicating direct liquid releases to the ocean were the dominant source, rather than deposition from the atmosphere.

B73. TEPCO [T6] and NRA [N20] conducted—and at the end of 2013 continue to conduct—seawater monitoring; they detected the presence of plutonium radioisotopes in seawater samples, but levels were near or below the detection limit.

(d) *Concentrations of ^{134}Cs and ^{137}Cs in sediments*

B74. Almost 1,000 samples of sediment from the surface (30 mm) of the seabed taken between the end of April 2011 and the end of 2012 off Fukushima Prefecture and neighbouring prefectures have been analysed [M11]. The radionuclides most frequently detected were ^{134}Cs and ^{137}Cs. The highest concentration of ^{137}Cs, of the order of 10^5 Bq/kg in dry sediment, was measured in the port of the FDNPS site. Levels decreased significantly with distance from the FDNPS site, with ^{137}Cs concentrations generally lying between 10 and 1,000 Bq/kg in dry sediment, compared to values of 1 Bq/kg before the accident (see figure B-XVIII). The initial ^{134}Cs/^{137}Cs ratio was close to 1, in line with ratios found in seawater. The higher concentrations were associated with fine sediments. Measurements performed on the 30–100 mm layer showed significant concentrations that could have resulted from bioturbation [O7]. The Committee considered how the distribution of ^{137}Cs in sediment developed with time, but it was difficult to draw conclusions, owing to the high spatial heterogeneity of concentrations. However, it was clear that concentrations of ^{137}Cs in sediment had changed much less over time compared to concentrations in water (compare figures B-XVII and B-XVIII).

B75. The resuspension of fine sediments in coastal areas is a process that recurs when currents and waves are sufficiently energetic. Transport of turbid layers generated by resuspension along the bottom can then redistribute radionuclides for several years before they are permanently buried under new layers of sediment. Moreover, sediment represents a source of radionuclides for marine species living or feeding on the ocean floor.

Figure B-XVIII. Concentrations of ^{137}Cs in sediment

Taken from [M11]. Higher values observed in the FDNPS port have not been plotted

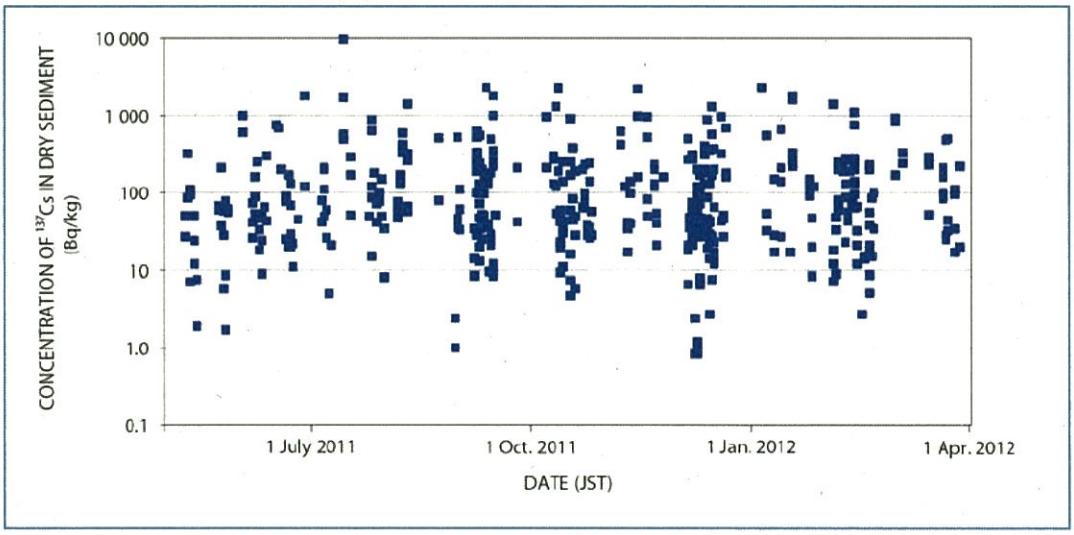

B. Marine dispersion models and validity checks

B76. The numerous observations available enabled an understanding of some of the characteristics of the dispersion of released radionuclides in the marine environment. Modelling of dispersion could supplement this understanding provided that models had been reasonably well-validated by observations. To understand how this dispersion occurred at the regional level, the modelled surface currents for the month of April 2011 are presented (as arrows) in figure B-XIX [E4]. This shows, in particular, the influence of the Kuroshio current that transports warm and salty waters along the

southern coast of Japan and then eastwards to the central Pacific Ocean north of the 35°N parallel. This current flows from about one hundred kilometres south of FDNPS and creates a boundary between the warm waters to the south and the cold waters to the north, into which the direct liquid releases of radionuclides were made. Periáñez et al. [P3] conducted similar modelling studies.

B77. Off the coast of FDNPS, the continental shelf (where the water is less than about 200 m deep—corresponding to the darker blue colours in figure B-XIX) is about 40 km wide. Currents on the continental shelf vary in response to forcing by the wind, tides and freshwater inputs from rivers. Wind seems to be the main driver of the currents in this coastal region. The coast induces a blockage which channels the currents within the first few kilometres. When the wind is favourable for southward transport, surface water and associated contaminants can reach the Kuroshio current within a few days, and then be dispersed eastwards towards the centre of the Pacific Ocean.

B78. To be confident in an analysis of the dispersion, the results of models had to be validated against available observations. The results of different models mentioned in section II.B of this appendix [E4, K3, T24] and those from the analysis of Periáñez et al. [P3] (which incorporated a dynamic model of the interactions between seawater and sediments) were compared with observations at different points. Masumoto et al. [M5] presented an intercomparison of the results of some of these models with others. The models sometimes related to winds used to force the hydrodynamic models, to oceanic currents, and to time series of concentrations at different points. Estournel et al. [E4], using the daily source term discussed in section II.B above, simulated the ^{137}Cs dispersion and then compared simulated and observed concentrations at 13 sites along the coast and at 3, 8, 15 and 30 km offshore (see position in the insert of figure B-XIX). The results are shown in figure B-XX. The variations of concentration with time were generally well reproduced, apart from the early observed increase in concentrations at 30 km offshore (discussed in section II.B of this appendix). This simulation was used to provide insight into how direct releases to the ocean and deposition from the atmosphere were dispersed in the ocean.

Figure B-XIX. Surface current simulated for April 2011 superimposed on the sub-marine topography (from [E4])[a]

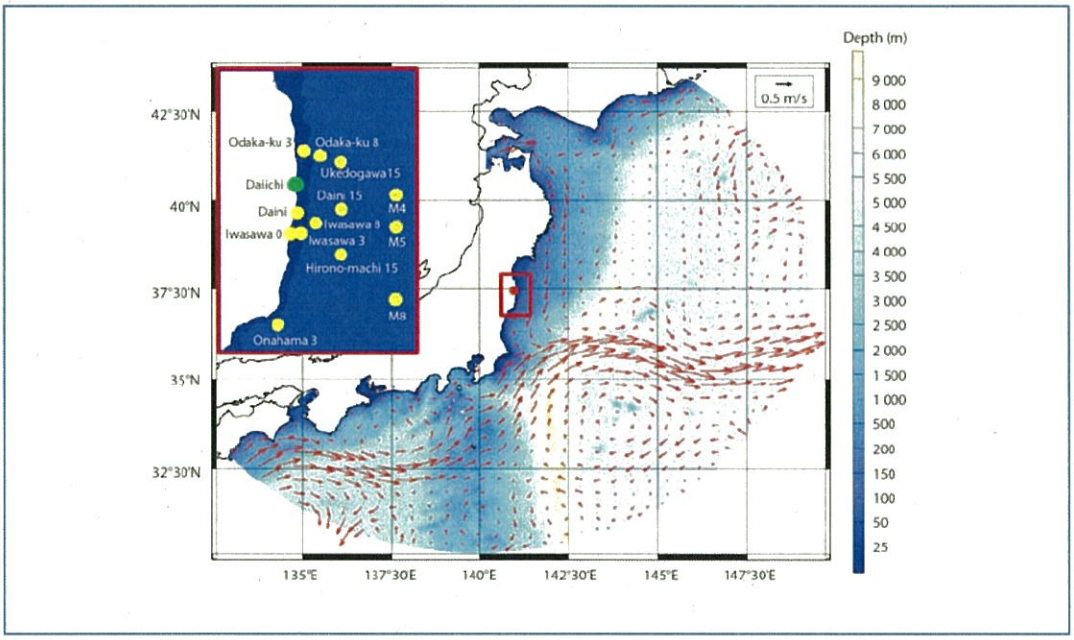

[a] *The red dot indicates the Fukushima Daiichi Nuclear Power Station (FDNPS). The top left insert is a close-up around FDNPS indicating the position of the points used to validate the dispersion model (see figure B-XX).*

Figure B-XX. Comparison of ^{137}Cs concentrations (Bq/L) observed (dots) and simulated (solid line) at different points indicated in the frames (from [E4])[a]

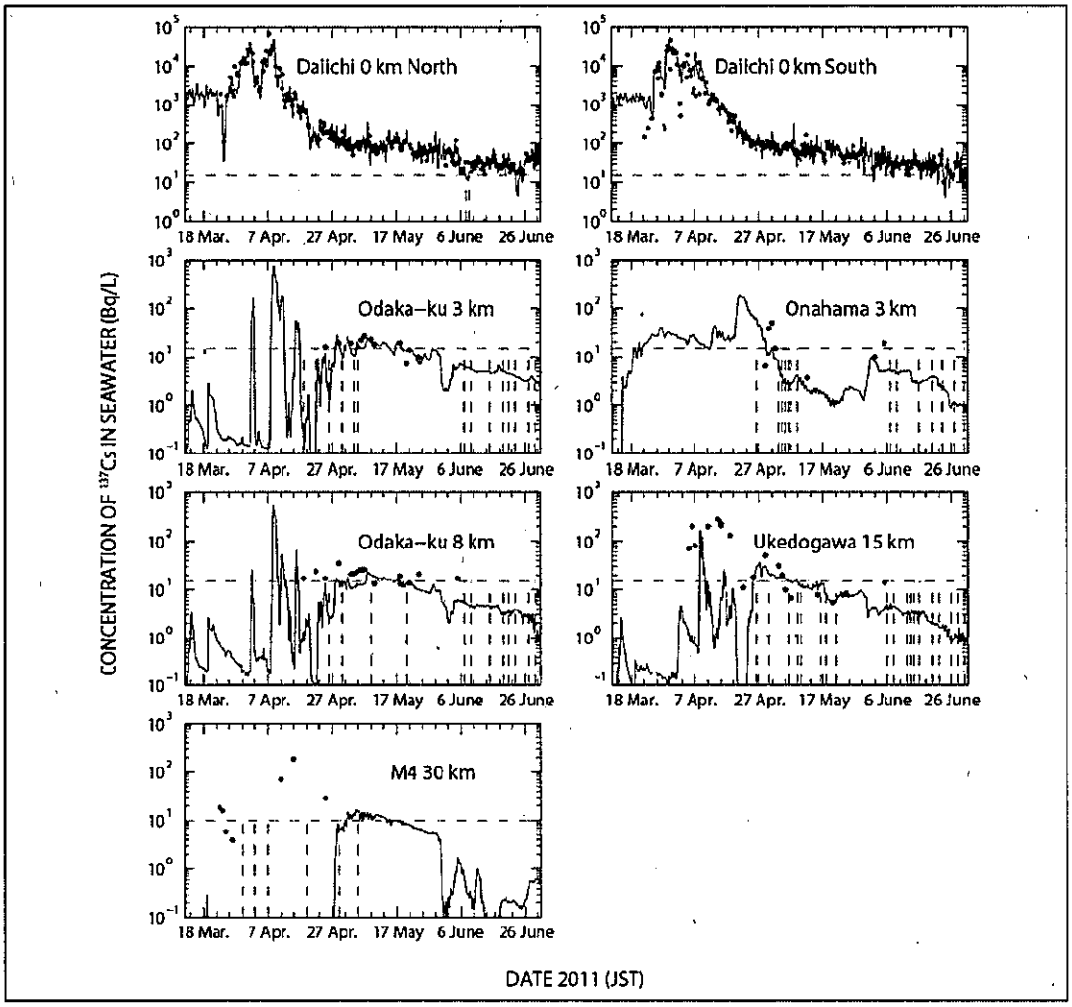

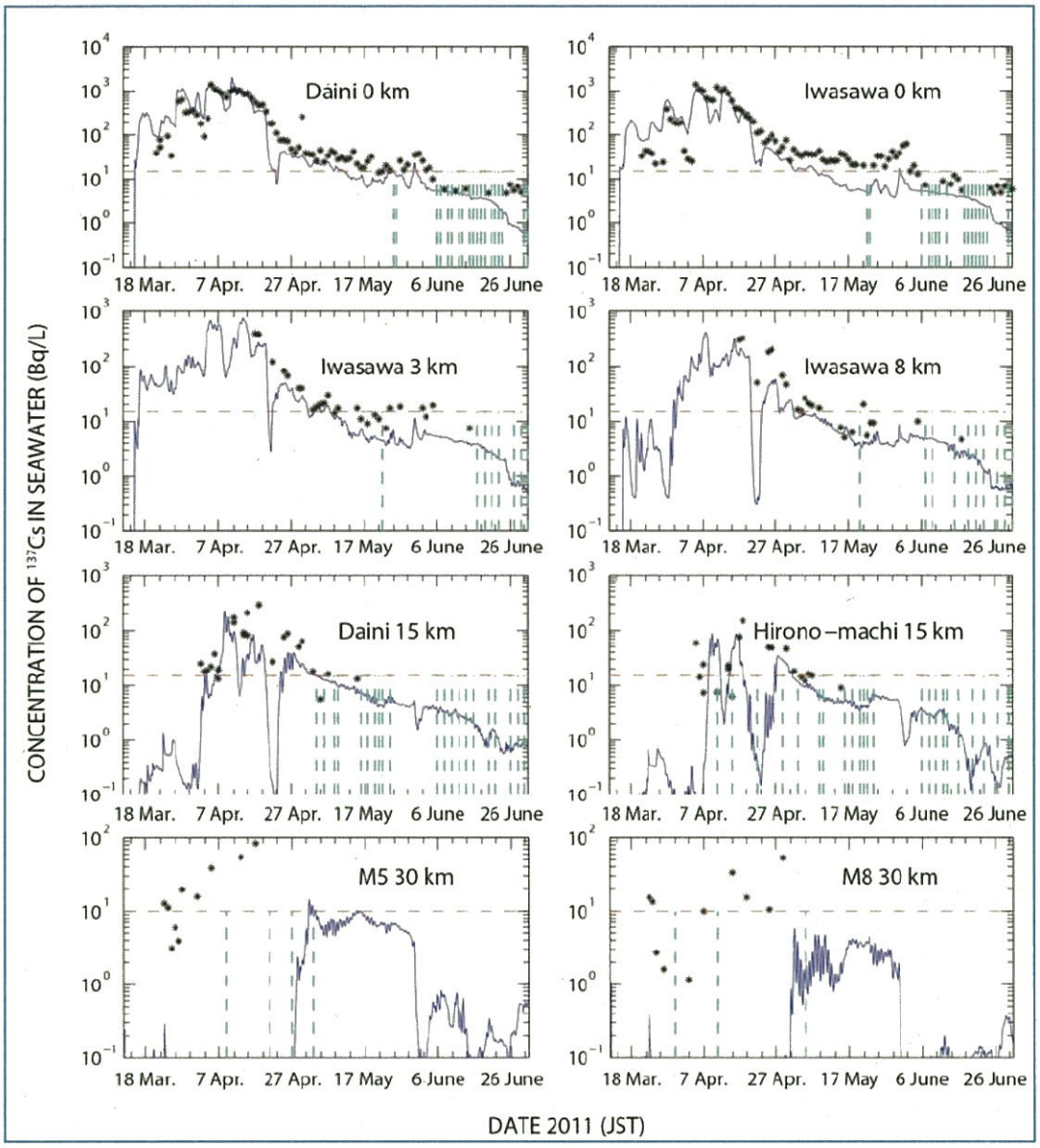

[a] See map on figure B-XIX for site locations. The red dashed line indicates the detection limit while vertical cyan dashed lines indicate observations below the detection limit.

C. Results of dispersion assessment

(a) *Dispersion of direct releases to the ocean*

B79. The wind blew mainly southwards during the first month after the accident, when the direct releases from FDNPS to the ocean were highest. Such wind conditions produced transport to the south and confinement against the coast (see figure B-XXI), owing to the Coriolis effect. This situation is typical of coastal downwelling. It is the origin of the high concentrations observed south of FDNPS (at Fukushima Daini Nuclear Power Station and Iwasawa beach) [T6]. This southward transport then led to

an interaction between the coastal waters carrying the released radionuclides and the Kuroshio current, and subsequently to an eastward transport.

B80. After mid-April, the wind blew mainly northwards inducing a northward and eastward surface current. This situation was favourable to disperse radionuclides in the entire coastal area, including to the north of FDNPS (see figure B-XXII). Radionuclide concentrations then decreased sharply near to the coast, while they increased 30 km offshore. An analysis of observations of ^{137}Cs and temperature and salinity profiles at 30 km offshore in mid-April indicated that radiocaesium was associated with a 10–20 m thick low-salinity layer. The presence of this river-influenced coastal water pushed by the wind over denser oceanic water promoted the offshore transport of radionuclides, limited their dispersion into the underlying waters and thereby increased the residence time of radionuclides in surface waters.

Figure B-XXI. Mean concentration of ^{137}Cs in surface waters (Bq/L) during the first month after the accident (from [E4])

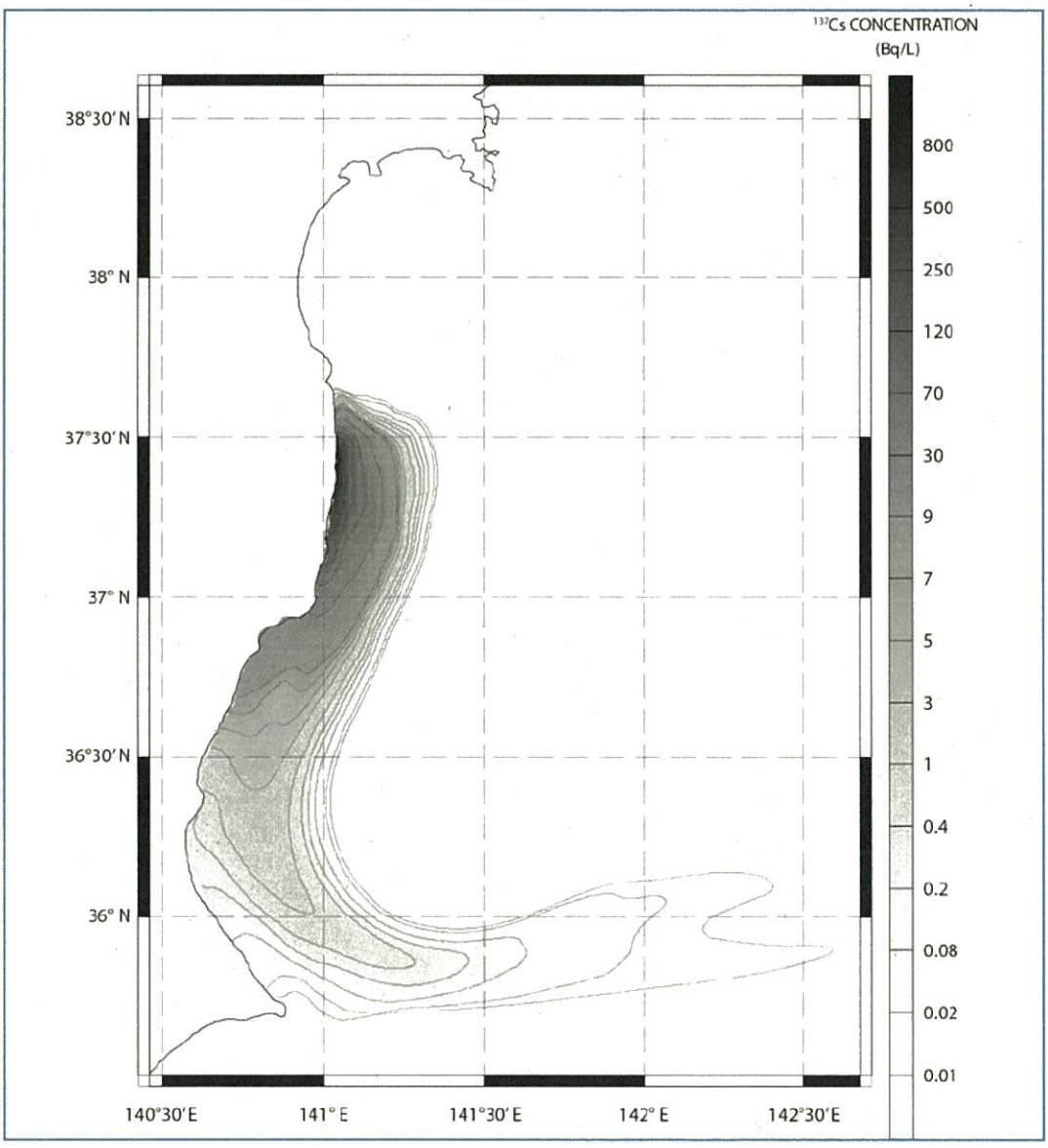

Figure B-XXII. Mean concentration of ^{137}Cs in surface waters (Bq/L) in May 2011 (from [E4])[a]

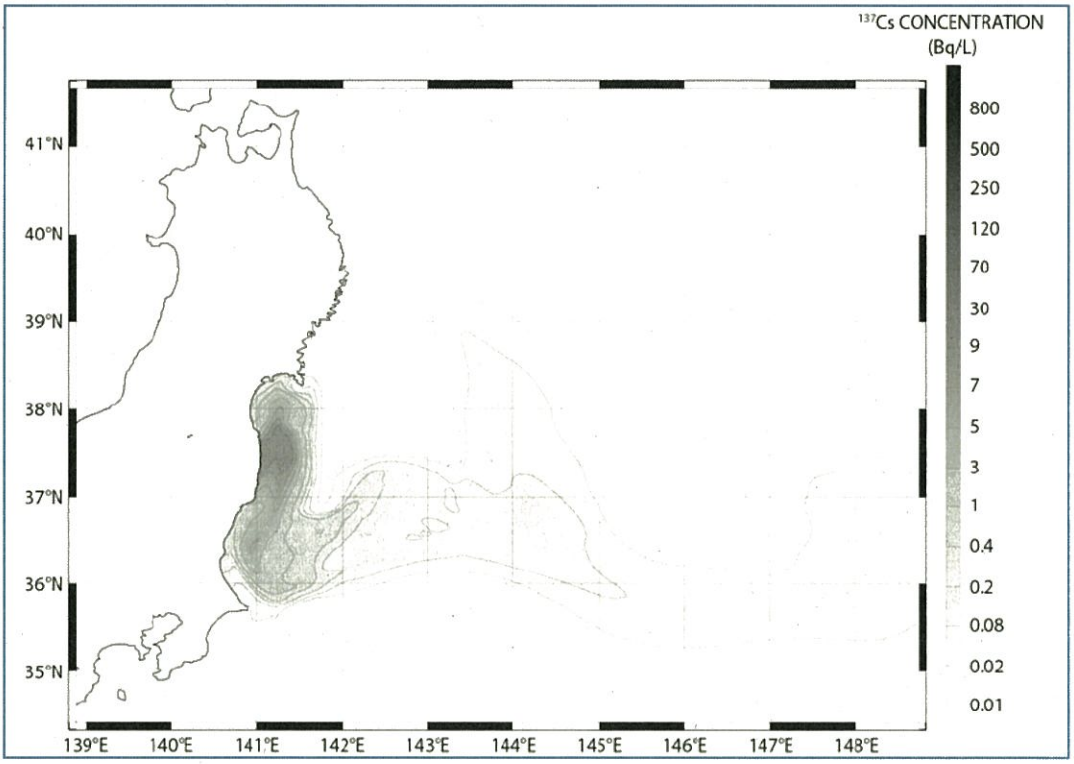

[a] *Note that the horizontal scale differs from the one used in figure B-XXI.*

(b) *Dispersion of radionuclides deposited from the atmosphere*

B81. Radionuclides released to atmosphere were deposited on to the ocean over a wide region. Deposition density was highest in the coastal area near FDNPS. According to different authors [E4, K3], the magnitude of the accumulated deposition density would have been of the order of 10^4 Bq/m^2 close to the coast and around 10^2–10^3 Bq/m^2 500 km away from FDNPS, depending on the wind direction at the time of the releases. Oceanic dispersion models have been used to simulate the fate of these deposits.

B82. The contribution to concentrations in surface waters due to these deposits from atmosphere was much lower than that due to the direct releases into the ocean (except perhaps during the first days, when direct releases were not detected). At large distances during the first month, atmospheric deposition was responsible for the observed concentrations, which were low (less than 0.05 Bq/L at a few hundred kilometres [E4]). These results were within an order of magnitude of the average observations reported by Honda et al. [H7], although some values around 0.3 Bq/L were measured in a relatively small area.

B83. Regarding ^{131}I, Kawamura et al. [K3] simulated concentrations along the coast south of FDNPS that reached a few hundreds of becquerels per litre in March, decreasing offshore to about 10 Bq/L also within March, and to 1 Bq/L in April.

(c) *Long-term global transport*

B84. Simulations of the ^{137}Cs dispersion across the Pacific Ocean over the first 30 years after the accident have been published [N3]. These simulations indicated that radionuclides released directly would reach the Californian coast of the United States 4–5 years after the accident, but this timescale was likely to have been overestimated because the low-resolution ocean model used in this study underestimated the strength of currents. This has been confirmed by observations reported by Aoyama et al. [A12] and discussed in section III.A of this appendix. However, the simulated concentrations for 2012 were of the same order of magnitude as Aoyama's observations. The model indicated that ^{137}Cs released directly from FDNPS would be distributed throughout the northern Pacific Ocean within ten years of the accident at concentrations below 10^{-3} Bq/L; these are less than concentrations of ^{137}Cs in the Pacific Ocean of $1–2 \times 10^{-3}$ Bq/L that existed before the accident [B25].

(d) *Uptake onto, and release from, sediments*

B85. Periáñez et al. modelled the interactions between seawater and sediments [P3] using a three-dimensional advection/diffusion model with terms describing the adsorption/desorption reactions between the deepest water layer and seabed sediments in a dynamic way using both one-step and two-step kinetic models. They estimated concentrations of ^{137}Cs in seawater and sediment for comparison with measurements. The model provided a fit to the measurements of ^{137}Cs concentrations in surface water similar to that illustrated in figure B-XX; it also was able to reproduce the general pattern of ^{137}Cs concentrations measured in sediments. The authors estimated a half-time for the ^{137}Cs content in the sediment of 167 days.